University of Alberta

Characterization and Evaluation of Methylcyclopentane and Cycylohexane Ring Opening of Ir/ZrO_2-MoO_3 Catalysts

By

Zhenhui Wang

A thesis submitted to the Faculty of Graduate Studies and Research in partial fulfillment of the requirements for the degree of *Master of Science*

In

Chemical Engineering

Department of Chemical and Materials Engineering

Edmonton, Alberta
Fall, 2006

Library and Archives Canada

Published Heritage Branch

395 Wellington Street
Ottawa ON K1A 0N4
Canada

Bibliothèque et Archives Canada

Direction du Patrimoine de l'édition

395, rue Wellington
Ottawa ON K1A 0N4
Canada

Your file Votre référence
ISBN: 978-0-494-22404-5
Our file Notre référence
ISBN: 978-0-494-22404-5

NOTICE:
The author has granted a non-exclusive license allowing Library and Archives Canada to reproduce, publish, archive, preserve, conserve, communicate to the public by telecommunication or on the Internet, loan, distribute and sell theses worldwide, for commercial or non-commercial purposes, in microform, paper, electronic and/or any other formats.

The author retains copyright ownership and moral rights in this thesis. Neither the thesis nor substantial extracts from it may be printed or otherwise reproduced without the author's permission.

AVIS:
L'auteur a accordé une licence non exclusive permettant à la Bibliothèque et Archives Canada de reproduire, publier, archiver, sauvegarder, conserver, transmettre au public par télécommunication ou par l'Internet, prêter, distribuer et vendre des thèses partout dans le monde, à des fins commerciales ou autres, sur support microforme, papier, électronique et/ou autres formats.

L'auteur conserve la propriété du droit d'auteur et des droits moraux qui protège cette thèse. Ni la thèse ni des extraits substantiels de celle-ci ne doivent être imprimés ou autrement reproduits sans son autorisation.

In compliance with the Canadian Privacy Act some supporting forms may have been removed from this thesis.

While these forms may be included in the document page count, their removal does not represent any loss of content from the thesis.

Conformément à la loi canadienne sur la protection de la vie privée, quelques formulaires secondaires ont été enlevés de cette thèse.

Bien que ces formulaires aient inclus dans la pagination, il n'y aura aucun contenu manquant.

Canada

ABSTRACT

The objective of this research was to study the activity and selectivity of ring opening reactions over Ir/ZrO_2-MoO_3 catalysts. MoO_3 was introduced by co-precipitation to stabilize ZrO_2. X-ray photoelectron spectroscopy (XPS) suggested that molybdenum and zirconium were present mainly in the form of MoO_3 and ZrO_2, respectively. X-ray diffraction (XRD) analysis indicated the structure of ZrO_2 underwent a transition of from monoclinic to tetragonal with increasing Mo content. In addition, the reducibility and acidity were also strongly related to the content of MoO_3. Iridium was incorporated by wet impregnation to a desired loading of 30 and 300 ppmw, with the concentration verified by instrumental neutron activation analysis (INAA). The vapor phase conversion of methylcyclopentane (MCP) and the liquid phase conversion of cyclohexane (CH) were subsequently studied to determine catalytic activity and selectivity. Iridium introduction greatly improved the conversion of MCP. The liquid-phase conversion of CH was carried in batch reactor. The catalyst with 3.5 at. % Mo and 30 ppmw Ir gave overall high activity and selectivity for the conversion of cyclohexane to n-hexane.

ACKNOWLEDGEMENTS

I am extremely grateful for the love, understanding, and support from my wife, Yanping Xu. I would also like to acknowledge my supervisor, Dr. Alan E. Nelson, for all of his advice, help, and encouragement.

I would like to thank all my past and present group members for their help and friendship, with special thanks to Carolyn Kenney for the excellent work she has done for this project. I am also grateful to the time and the assistance provided by Wayne Moffat, Dr. John Duke, Dr. Murray Gray, Andree Koenig, Walter Boddez, Richard Cooper, Dimitre Karpuzov and Shihong Xu.

I would also like to acknowledge Syncrude Canada Ltd. and NSERC for their funding.

Table of Contents

CHAPTER 1 INTRODUCTION
1.1 General Introduction 1
1.1.1 Oil Sands in Alberta 1
1.1.2 Technologies and Catalysts 2
1.2 Research Objectives 4

CHAPTER 2 LITERATURE REVIEW
2.1 Environmental Regulations 5
2.1.1 Diesel Fuel Quality and Specifications 5
2.1.2 Cetane Number 6
2.1.3 Aromatic Compounds and Cetane Number 6
2.1.4 Strategies for improving cetane number 7
2.2 Selective Ring Opening (SRO) 8
2.2.1 Mechanisms of Selective Ring Opening 8
2.2.2 Hagg-Dessau Ring Opening Catalysts 11
2.2.3 Bifunctional Ring Opening Catalysts 11
2.2.3.1 Zeolite Supported Platinum Group Metals 12
2.2.3.3 Effect of Reaction Conditions 15
2.2.4 Model Compounds 18
2.3 Properties of ZrO_2-Based Catalysts 20
2.3.1 Structure of Zirconia 20
2.3.2 Stabilization of Zirconia 20
2.3.3 Catalytic Activity of Zirconia Supported Catalysts 21
2.3.4 ZrO_2 as a Ring Opening Catalyst 22
2.3.4.1 Effect of Mo Incorporation 22
2.3.4.2 Effect of Iridium Incorporation 23
2.4 Summary 24

CHAPTER 3 EXPERIMENTAL METHODS
3.1 Catalyst Preparation 26
3.1.1 Chemicals 26
3.1.2 Synthesis of ZrO_2-MoO_3 27
3.1.3 Iridium Impregnation 28
3.2 Catalyst Characterization 29
3.2.1 X-Ray Photoelectron Spectroscopy (XPS) 29
3.2.2 Instrument Neutron Activation Analysis (INAA) 31
3.2.3 X-Ray Diffraction 34
3.2.4 Temperature Programmed Techniques 35
3.2.4.1 Introduction to the AutoChem II 2920 36
3.2.4.2 Temperature Programmed Reduction (TPR) 38
3.2.4.3 NH_3 Temperature Programmed Desorption (TPD) 39
3.2.4.4 CO Chemisorption 41
3.2.4.4 BET Surface Area 42
3.3 Catalytic Reaction 44

3.3.1 Chemicals 44
3.3.2 Pulse Mode 44
3.3.3 Reaction in Batch Reactor 45
3.3.3.1 Procedure 46
3.3.3.2 Products Analysis 48

CHAPTER 4 RESULTS
4.1 X-Ray Photoelectron Spectroscopy 50
4.2 Instrument Neutron Activation Analysis (INAA) 55
4.3 X-Ray Diffraction 57
4.4 Results of Temperature Programmed Techniques 60
4.4.1 Temperature Programmed Reduction (TPR) 60
4.4.2 NH_3 Temperature Programmed Desorption (TPD) 62
4.4.3 CO Chemisorption 68
4.4.4 BET Surface Area Measurement 70
4.5 Catalytic Activity and Selectivity 71
4.5.1 Methylcyclopentane Conversion 71
4.5.2 Cyclohexane Convesion 74

CHAPTER 5 DISCUSSION
5.1 X-Ray Photoelectron Spectroscopy (XPS) 79
5.2 X-Ray Diffraction 80
5.3 Temperature Programmed Techniques 81
5.3.1 Temperature Programmed Reduction (TPR) 81
5.3.2 NH_3 Temperature Programmed Desorption (TPD) 82
5.3.3 CO Chemisorption 83
5.3.4 BET Surface Area Measurement 85
5.4 Catalytic Activity and Selectivity 86
5.4.1 Reaction Pathways 86
5.4.2 Pulse Mode (MCP) 88
5.4.3 Batch Mode (MCH) 90

CHAPTER 6 CONCLUSION
6.1 Conclusion 95
6.2 Future Work 97

REFERENCES 98

List of Tables

2.1 Comparison of Ring-Opening Pathways.....9

3.1 List of Chemicals.....26

3.2 Sample list with different Mo atomic concentration.....28

4.1 XPS results of Ir/ZrO_2-MoO_3 catalysts.....54

4.2 Iridium concentration determined by INAA technique.....56

4.3 Desorbed amount of ammonia for different acid sites on Ir/ZrO_2-MoO_3.....66

4.4 Heat of desorption for different acid sites in Ir/ZrO_2-MoO_3 catalysts (300 ppmw Ir).....68

4.5 Iridium dispersion for Ir/ZrO_2-MoO_3 catalysts.....69

4.6 BET surface area results for catalysts with Ir at 300 ppmw level.....71

4.7 Comparison of conversion results for catalysts with and without Ir.....74

List of Figures

2.1 Cetane numbers of various compounds.....7

2.2 Bifunctional mechanisms for methylcyclohexane ring opening.....10

3.1 General Principle of INAA.....32

3.2 AutoChem II 2920.....37

3.3 Experiment Setup in Sand Bath.....47

4.1 XPS Survey Scan for catalyst with 1 at. % Mo.....52

4.2 XPS High Resolution Scan for catalyst with 1 at. % Mo.....53

4.3 High-resolution XRD Patten for ZrO_2 - MoO_3 without Ir Catalysts.....59

4.4.A XRD patterns of MoO_3/ZrO_2 catalysts obtained by co-precipitation and calcined at 500°C (●) Tetragonal ZrO_2; (■) monoclinic ZrO_2.....60

4.4.B XRD pattern of catalysts with low Mo loading.....60

4.5 TPR profile of Ir/ZrO_2-MoO_3 catalysts.....62

4.6 NH_3 TPD profile of Ir/ZrO_2-MoO_3 catalysts at 45 °C/min.....65

4.7 NH_3 TPD profile of 0 at. % Mo at different heating rate.....67

4.8 CO chemisorption profile of 5 at. % Mo catalyst.....70

4.9 Products GC Spectrum for catalyst with 0.7 at. % Mo and 38 ppmw Ir.....77

4.10 Selectivity to n-hexane as function of catalyst composition (400 °C, 7 MPa H_2).....78

4.11 Activity as function of catalyst composition (400 °C, 7 MPa H_2).....79

5.1 UPS patterns for CO in the gas phase, bonded to an iridium cluster, and adsorbed on an iridium surface.....85

5.2 Classical bi-functional mechanism for selective ring opening.....88

5.3 Haag-Dessau mechanism for selective ring opening.....89

5.4 Ring opening reaction for MCP on ZrO_2/MoO_3.....90

5.5 Classical bi-functional mechanism for CH on Ir/ZrO_2-MoO_3.....93

Nomanclature

AAS – Atomic Adsorption Spectroscopy

AECL – Atomic Energy of Canada Limited

AutoChem – Automated Chemisorption

BCH - Butylcyclohexane

BE – Binding Energy

BET – Brunauer Emmett Teller

CH – Cyclohexane

CN – Cetane Number

EPA – Environmental Protection Agency

HDN – Hydrodenitrogenation

HDS – Hydrodesulfurization

HYD – Hydrogenation

ICP-AES – Inductively Coupled Plasma-Atomic Emission Spectroscopy

INAA – Instrument Neutron Activation Analysis

MCH - Methylcyclohexane

MCP – Methylcyclopentane

MS – Mass Spectrometry

NSLS - National Synchrotron Light Source

PCP - Pentylcyclopentane

ROP – Ring Opening Products

RSF – Relative Sensitivity Factor

SRO – Selective Ring Opening

TCD – Thermal Conductivity Detector

TOF – Turnover Frenquency

TPD – Temperature Programmed Desorption

TPR – Temperature Programmed Reduction

TTZ – Tetragonal Toughened Zirconia

TZP – Tetragonal Zirconia Polycrystal

XPS - X-ray Photoelectron Spectroscopy

XRD - X-ray Diffraction

2MP – 2-methyl-pentane

3MP – 3-methyl-pentane

CHAPTER 1

INTRODUCTION

1.1 General Introduction

1.1.1 Oil Sands in Alberta

Oil sands are unconventional oil and crude deposits that are substantially heavier (more viscous) than other crude oils. Oil sands consist of sand, bitumen, mineral rich clays and water. Bitumen is extracted from the oil sands and is subsequently upgraded into a synthetic crude oil to make it transportable by pipelines and usable by refineries (http://www.energy.gov.ab.ca/docs/oilsands/pdfs/osgenbrf.pdf).

Alberta's large oil sands deposits (140,800 square kilometers) are contained in three different areas: Peace River, Athabasca (Fort McMurray area), and Cold Lake (north of Lloydminster). These oil sands deposits contain approximately 1.6 trillion barrels of bitumen, of which 174 billion barrels are proven reserves that can be recovered using current technology (http://www.energy.gov.ab.ca/docs/oilsands/pdfs/osgenbrf.pdf).

According to previously published reports, Alberta's oil sands accounted for approximately 52.7 percent of Alberta's total crude oil and equivalent production, and about 34.8 percent of all crude oil and equivalent produced in Canada in 2003 (http://www.energy.gov.ab.ca/docs/aboutus/pdfs/Alberta_Energy_Overview.pdf). Annual oil sands production is growing steadily. Output of commercial oil sands production increased to 858,000 barrels per day (bbl/d) in 2003 from 741,000 bbl/d in 2002. In 2005, Alberta's oil sands production accounted for one-half of Canada's total crude output and 10 per cent of North American production (http://www.energy.gov.ab.ca/89.asp). Indeed,

Alberta's oil sands reserves were described by Time Magazine as "Canada's greatest buried energy treasure" and "could satisfy the world's demand for petroleum for the next century." (http://www.alberta-canada.com/economy/naturalAdvantages/energy.cfm).

Upgrading is the crucial step in changing Alberta oil sands bitumen from a black tar substance with high viscosity into a synthetic crude oil, such that oil refineries can process the upgraded bitumen into liquid fuels. Many upgrading projects have been proposed and launched in Western Canada to accommodate the increased utilization of Alberta's oil sands. The upgrading capacity has experienced an increase from 339,000 bbl/day in 1996 to 733,000 bbl/day in 2004 (http://www.capp.ca/raw.asp?x=1&dt=NTV&e=PDF&dn=34093).

1.1.2 Technologies and Catalysts

In Alberta oil sands bitumen, the content of aromatic compounds is relatively high, and it has been proven that the aromatic content has a close relationship with the fuel quality and the formation of harmful emissions during fuel combustion (Du et al., 2005). The amount of particulates during diesel combustion can be reduced by lowering the aromatics content and increasing the cetane number. Therefore, removal of aromatics has become a key process in the bitumen upgrading industry to respond the more restrictive environmental standards and legislation.

In the upgrading and refining industries, hydroprocessing can be categorized into two aspects according to different purposes (Eliche-Quesada, 2004). In hydroconversion, the structure and molecular weight of organic compounds is changed by hydrogenation,

hydrocracking, isomerization, and dearomitization. On the other hand, hydrotreating eliminates hetero-atoms, namely sulfur and nitrogen.

Currently, mild hydrocracking is used to improve the quality of fuel by increasing the ignition properties, i.e. low cetane number in diesel fuel and high smoke point in jet fuel (Eliche-Quesada, 2004). It this process, a reaction is carried out under hydrogen pressures lower than that for typical hydrocracking but at a higher temperature than that for hydrotreating. However, the extent of aromatic hydrogenation is still not sufficient to produce a diesel fraction with an acceptable cetane number. Therefore, a two-stage process has been designed and applied in many refineries worldwide (Song et al., 2003). This type of process includes deep hydrodesulfurization (HDS) in the first stage, and aromatic saturation and ring opening over the noble metal catalysts in the second stage.

The catalyst plays a very critical role in aromatic saturation and ring opening. Therefore, the development of a highly active and selective catalyst is a potentially useful method to produce a high-quality diesel fuel. Conventional sulfide catalysts, i.e. NiMoS, demonstrate very high activity in hydrodesulfuration and hydrogenation reactions (Weisser et al., 1973) and are usually used for feedstocks that contain an appreciable amount of sulfur and nitrogen, while supported noble metal catalysts are used for sulfur- and nitrogen-free feedstocks. This difference is due to the high sulfur deactivation susceptibility of noble metal catalysts; however, an acidic support, such as an acidic zeolite, can enhance the sulfur resistance of a noble metal catalyst (Cooper et al. 1996).

Solid-acid supported noble metals catalysts, or bifunctional catalysts, have been extensively studied for aromatic hydrogenation and ring opening, and several reaction mechanisms have been proposed (McVicker et al., 2002; Arribas et al., 2002; Arribas et

al., 2004; Santikunaporn et al., 2004). McVicker et al. (2002) summarized a comprehensive investigation about selective ring opening of naphthenic molecules. The activity and selectivity of several catalysts were compared, and Ir/Al_2O_3 was shown to be the most active catalyst for unsubstituted C-C bonds in cyclopentanes and bicyclonaphthenes.

1.2 Research Objectives

The objective of this research is to synthesize and study a new bifunctional catalyst to significantly increase the catalytic activity and selectivity for ring opening reactions. These catalysts are comprised of iridium supported on stabilized ZrO_2. The tetragonal polymorph of ZrO_2 is stabilized using varying amounts of MoO_3. In order to produce desirable products with a high cetane number, catalysts with different Ir and MoO_3 loading have been prepared and evaluated.

A detailed literature review is given in Chapter 2. This chapter discusses environmental regulations, the mechanisms of selective ring opening and properties of ZrO_2 based catalysts. In Chapter 3, a complete description about the techniques applied to characterize the acidic and metallic functions of catalysts is presented, and the details for methylcyclopentane and cyclohexane catalytic activity experiments are summarized. Chapter 4 presents the experimental results, including characterization and the activity and selectivity for methylcyclopentane and cyclohexane ring opening for the various catalysts studied. Chapter 5 compares, analyzes and discusses the results, and the conclusions and suggested future work from this study are summarized Chapter 6.

CHAPTER 2

LITERATURE REVIEW

2.1 Environmental Regulations

Diesel and gasoline engines emit a significant amount of pollutants, and more stringent standards for gasoline and diesel-powered vehicles are being proposed and established by the U.S. Environmental Protection Agency (EPA) to regulate emissions.

2.1.1 Diesel Fuel Quality and Specifications

The Reformulated Gasoline Program Phase II was adopted on January 1, 2002, and specifies the reduction of aromatics by 22 % (http://www.epa.gov). In 2004, the EPA issued new specifications requiring that a minimum cetane number (CN) of 40 and maximum aromatics content at 35 vol. % must be met by June 2006. Additionally, emission regulations specified by the European Union require a minimum diesel cetane number of 51 and an average cetane number of 55 is being considered (http://www.dieselnet.com/standards/eu/ld.html). In order to meet these increasingly stringent standards, new diesel fuel processing technology must be developed.

Meanwhile, the quality of crude oil feedstock is being reduced because it is heavier with increasing amounts of heteroatoms. The API gravity of processed crude in the U.S. declined 0.12 °/year between 1997 and 2001 (US Energy Information Administration, 2005), and this trend is expected to continue for the foreseeable future.

Canada's oil sands have been widely recognized as new source to satisfy the crude oil demands of the world. Bitumen production is estimated to be 5.6 million bbl/d by

2020. However, the synthetic crude oil derived from bitumen possesses very high aromaticity, which causes low cetane number and poor ignition quality of diesel fuel. In order to utilize oil sands bitumen and meet stringent emission standards, new process and catalysts are required.

2.1.2 Cetane Number

The cetane number (CN) is defined as a measurement of ignition quality of diesel fuel, whereby a fuel with a high cetane number has higher autoignition characteristics when injected into a compression ignition (CI) engine. Cetane number is determined by an engine test using two reference fuel blends of known cetane numbers. The reference fuels are prepared by blending normal cetane (n-hexadecane), having a CN of 100, with heptamethylnonane, having a value of 15 (http://www.dieselnet.com/gl-a.html). The cetane number of a fuel is thus characterized as having the same ignition quality of a mixture of n-hexadecane and heptamethylnonane.

2.1.3 Aromatic Compounds and Cetane Number

Aromatic compounds in petroleum can be classified into four groups; monoaromatics, diaromatics, triaromatics, and polycyclic aromatics. Among these compounds, the polycyclic aromatics with four or more benzene rings are mainly found in high boiling distillate fractions, while the other three types are significant components of middle distillates.

The concentration of aromatics is associated with cetane number, whereby the reduction of aromatics can significantly increase the quality of diesel fuel. In Figure 2.1,

the cetane number is increased from 5 to 35 when naphthalene is completely saturated to form decalin. However, this conversion in itself is not sufficient and does not satisfy new fuel standards because the cetane number of decalin is still low. However, if ring opening further proceeds by cleaving an endocyclic C-C bond to produce to C_4-cyclohexane, a cetane number of 60 can be obtained (Arribas et al., 2004), which would meet the new fuel specifications. Therefore, the aromatic saturation and selective ring opening mechanism in Figure 2.1 presents a possible method to increase diesel fuel quality.

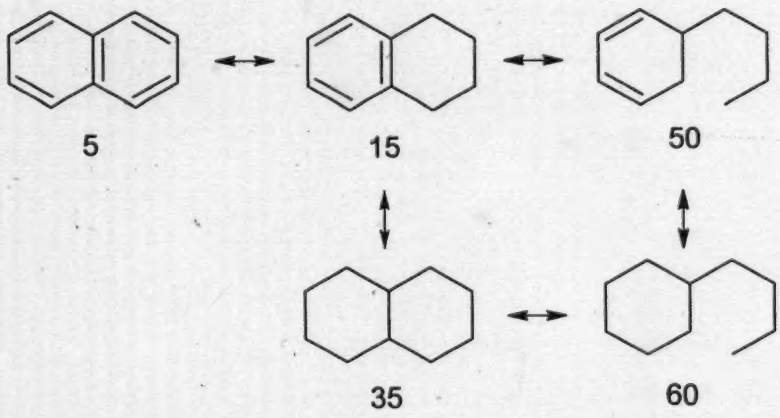

Fig. 2.1 Cetane numbers of various compounds (adapted from Arribas et al., 2004)

2.1.4 Strategies for improving cetane number

In order to satisfy the new requirements for diesel cetane number, several approaches have been suggested. One such method is to introduce "cetane boosters," which are frequently organic nitrate compounds (Lee et al., 1993). On the other hand, cetane boosters increase the chance of more dangerous ultra-fine particle emissions (AD Bank, 2003). Mixing a low CN fuel with Fischer–Tropsch (FT) gas-to-liquids diesel fuel

is another way to increase the CN and reduce aromatics content (Knottenbelt, 2002); however, this has been proven a costly solution (McCormick et al., 2003).

Another option to obtain higher CN is fully saturating aromatics, but the improvement of cetane number depends on the nature of feedstock (McVicker et al., 2002). As shown in Figure 2.1, aromatics saturation combined with selective ring opening is effective to significantly improve CN than aromatic saturation alone. Thus, selective ring opening suggests a new route to satisfy the stricter diesel fuel quality requirements.

2.2 Selective Ring Opening (SRO)

Selective ring opening (SRO) is described as opening naphthene rings without loss of reactant molecular weight, which means that only one endocyclic C-C bond for each aromatic ring is broken, thus preventing significant molecular weight reduction.

2.2.1 Mechanisms of Selective Ring Opening

It is widely recognized that selective ring opening based on bifunctional catalysis procees via a two-step reaction. The first process is isomerization (ring contraction) from a six-membered ring to a five-membered ring, and the second step is endocyclic C-C bond scission. For example, Kubicka et al. (2004B) found that almost no ring opening products (ROP) were obtained when decalin was at its highest concentration, which suggested that the ring opening products was related to the concentration of isomers instead of starting materials.

Three different reaction mechanisms for the ring opening of naphthenes, including free radical, carbocation, and hydrogenolysis, have been extensively discussed in the literature. McVicker and co-workers (2002) compared and discussed these pathways in their previous study. The characteristics of the three primary mechanisms for the ring opening of naphthenes are summarized in Table 2.1.

Table 2.1 Comparison of Ring-Opening Pathways (adapted from McVicker et al., 2002)

Primary conversion route	Catalyst type	Naphthene ring/alkane (side chain) bond cleavage ratio
Free radical	None—thermal	<1.0
Carbocation	Solid acids	<<1.0
Hydrogenolysis	Metals	>1.0

The free radical reaction pathway is initiated by adding radical initiators at high temperature, and the yields of ring opening products are usually limited due to competing reactions (McVicker et al., 2002).

The second possible pathway, carbocation ring cleavage, is catalyzed by the presence of a solid acid. The reaction is initiated by an olefin intermediate produced by dehydrogenation of naphthene molecules, or a cationic species by hydride abstraction, and followed by β-scission. Because the rate of β-scission in endocyclic naphthene rings is two or three orders of magnitude slower that that in exocyclic scission, this mechanism consequently results in low SRO products (McVicker et al., 2002).

The last mechanism, hydrogenolysis, is usually performed using supported metals to facilitate naphthene ring C-C bond cleavage. For selective ring opening, only one

endocyclic C-C bond is required to break (McVicker et al., 2002), and further C-C bond scission results in molecular weight reduction.

Raichle et al. (2001) discussed in detail the classical bifunctional mechanism, and a schematic of this mechanism is presented in Figure 2.2.

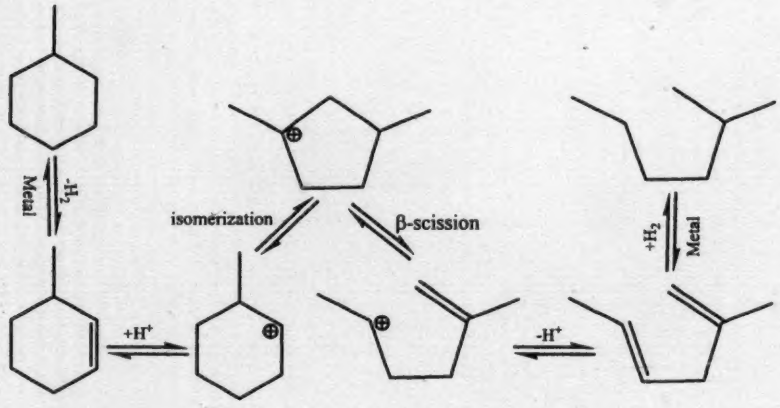

Fig. 2.2 Bifunctional mechanisms for methylcyclohexane ring opening (Adapted from Raichle et al., 2001)

In this mechanism, an alkylcycloalkane (methylcyclohexane) is dehydrogenated on the metal sites to form an unsaturated species, and then the species is protonated to produce alkylnaphthene carbonium ions on acidic sites. The carbonium ions can undergo isomerization followed by β-scission to cleave the C-C bond. The resulting olefin is hydrogenated on the metal sites to obtain ring opening products.

2.2.2 Hagg-Dessau Ring Opening Catalysts

In addition to the aforementioned ring opening mechanisms, when the noble metal concentration is very low, a Hagg-Dessau mechanism could prevail during the ring opening reaction. Raichle et al. (2001) proposed this mechanism for methylcyclohexane ring opening following the observation that the selectivity to C_{2+}-n-alkanes was high when methylcyclohexane was reacted on H-ZSM5 catalysts with a small amount of Pd. The methylcyclohexane was suggested to undergo protonation to form a transitional carbonium ion on acidic sites without undergoing dehydrogenation as in a bifunctional mechanism. The justification for this pathway was that there were insufficient metal sites and this limited the dehydrogenation activity.

The catalytic properties of Hagg-Dessau catalysts are closely correlated to temperature (Raichle et al. 2001). High temperature usually favors selectivity to n-alkanes, because Hagg-Dessau ring opening is very energy demanding (Abraham, 2005).

2.2.3 Bifunctional Ring Opening Catalysts

Although ring opening can be accomplished on either acidic or metallic catalysts, it is widely recognized that it is much more effective to combine the two types of active sites. The acidic sites facilitate the isomerization from six-membered rings to five-membered rings, and consequently promote the ring opening on metallic sites. These dual function catalysts are commonly referred to as bifunctional catalysts.

The catalyst morphology can influence the yield and product distribution. The support is important in order to obtain not only a high dispersion of active metal but also to allow the access of molecules through pores to the active centers. Many efforts have

been devoted to investigating the role of pore size, which affects the diffusion of the largest molecules.

2.2.3.1 Zeolite Supported Platinum Group Metals

Zeolites are the most commonly used acidic supports for bifunctional ring opening catalysts. Zeolites are three-dimensional, microporous, crystalline solids with well-defined structures that contain aluminium, silicon, and oxygen in their regular framework; cations and water are located in the pores. The silicon and aluminium atoms are tetrahedrally coordinated with each other through shared oxygen atoms. Another special aspect about zeolites is that the pore and channel sizes are nearly uniform, allowing them to act as molecular sieves (http://www.lenntech.com/zeolites-structure-types.htm).

Selective ring opening is usually carried using noble metals catalysts, including Pt, Pd, Ir, Ru and Rh, supported on solid acids. Arribas et al. (2004) reported the role of the metal site in Pt(Ir)/USY during tetralin hydrogenation and ring opening. The introduction of Pt significantly increased the rate of isomerization, and then the formation of ring opening products, compared to a monofunctional USY catalyst. The yield of ROPs increased with the increasing distance between acidic sites and Pt, and with increasing Pt loading in the range of 0.25-4 wt. %. They also observed that Ir/USY did not result in an increase of ROPs as compared to the Pt/USY catalyst.

Kubicka and co-workers (2004A) investigated a relationship between the acidity and structures of H-Beta, H-Y and H-MCM-41 zeolites, and their activity and selectivity for the ring opening of decalin. The presence of Bronsted acid sites was crucial for both

isomerization and ring opening, and they believed that isomerization was required for decalin ring opening. That is, decalin must be isomerized to produce alkyl-substituted bicyclononanes to make ring opening proceed and the concentration of Bronsted acid sites was strongly related to the catalyst activity. Generally speaking, a higher acidity led to higher activity.

Kubicka et al. (2004B) also studied the change of activity and selectivity of the catalysts in the ring opening of decalin at 473-543 K using Pt supported on H-Beta, H-Y and H-Mordenite zeolites. They found that the activity of the proton-form was increased significantly with Pt addition. Yields of ROPs as high as 30 mol % were achieved compared to only 8 mol % of ROPs on the proton-form of zeolites without platinum. The addition of platinum also affected the product distribution. Yields of cracking and heavy products decreased, and they attributed these changes to the interaction between Bronsted acid sites and platinum.

Walter et al. (1995) used methycyclohexane (MCH) and n-hexane (n-CH) as model compounds to investigate competitive reactions over alumina-supported platinum, iridium and ruthenium catalysts. They observed that ROP selectivity of MCH reached up to 50 % on Ru catalysts, which was shown to be dependent on particle size. Only the reaction for the dehydrogenation to toluene was found on Pt catalysts regardless of what the particle size was.

Bimetallic catalysts for ring opening have also been reported, including Pd-Pt bimetallic catalysts supported on various zeolites, such as USY zeolite, HY zeolite, and HL zeolite (Yasuda et. al., 1997; Yasuda et al., 1999; Lebihan et al., 2002). Jacquin et al. (2004) reported a type of bimetallic catalyst for improving the cetane number of diesel

fuel based on Pt-Pd. Pt and Pd were incorporated into a mesoporous aluminosilicate by three different methods, including direct incorporation, impregnation of metallic solution into the support and ion exchange. Impregnation and ion change methods gave more uniform intermetallic Pt-Pd particles size than direct incorporation. The introduction of Pd enhanced the single-metal catalyst ability to sulfur resistance.

The impact of USY zeolite acidity to the coupled hydrogenation and ring opening reaction were reported by Arribas et al. (2002). They found that product yields and selectivities for 1-methylnaphthalene were strongly related to the zeolite acidity. The selectivity of the C11 fraction, which was the selective ring opening product and determined the quality of products, increased with the decreasing density of Bronsted acidic sites at the same reaction temperature. Arribas and co-workers (2004) also investigated another Pt-containing bifunctional catalyst supported on the new ITQ-21 zeolite, which has a large pore structure. It has been previously highlighted that larger pore structure zeolites had higher activity (Corma et al., 2001). Arribas et al. (2004) proved that the bifunctional catalyst of Pt/ITQ21 had excellent activity for the hydrogenation and ring opening of tetralin (250-325 °C, 3.0 MPa). When the density of Bronsted acid sites was decreased, the maximum ROP yields shifted from 300 °C to 350 °C. Additionally, a conclusion was drawn that the maximum yield of ROPs with Pt/ITQ21 was around 25 % and 40 % higher than that in Pt/USY and Pt/Beta, respectively, using the same temperature and similar acid site density. They believed that this resulted from the larger pore size in ITQ-21, such that ROPs diffused out from pores very easily.

Additional studies regarding the role of acidity have been performed. For example, Santikunaporn et al. (2004) studied decalin and tetralin ring opening over HY and Pt/HY zeolite catalysts by changing the acidity. HY zeolites were very effective for ring contraction and ring opening if the density of acid sites was well controlled, that is not too high or too low. Kustov et al. (2001) studied NiW/HY catalysts and reported that the acidic function was beneficial for multiple-ring compounds compared to single ring ones compounds.

For Pt catalysts, the selectivity of MCP ring opening strongly depends on the metal particle size (Kramer et al., 1983; Kramer et al., 1984). Small Pt particle size favored a non-selective mechanism and promotes a statistic ratio of products, which are 2MP, 3MP, n-hexane. On the other hand, increasing Pt loading produced the formation of 2MP and 3MP, but restricted n-hexane. Pt/Al_2O_3 and Rh/Al_2O_3 have shown a close relationship with particle size in the hydrogenolysis of cyclopentane, and the activity increased with particle size (Gault et al., 1981; Che et al., 1989). Pd/Al_2O_3 exhibited an opposite tendency, and the activity of Ir/Al_2O_3 could not be correlated to particle size.

In general, it has been widely recognized that bifunctional catalysts, consisting both acidic and metallic sites, are ideal candidates to catalyze selective ring opening to improve the quality of diesel fuel.

2.2.3.3 Effect of Reaction Conditions

Ring opening is strongly dependent on reaction temperature. From a thermodynamic perspective, the hydrogenation of aromatic compounds is reversible and

exothermic, and therefore, decreasing the temperature will increase the rate constant and favor the reactions.

Several studies have reported the ring opening of MCP at a temperature range from 468 to 513 K (Teschner et al., 2000; Teschner et al., 2003). In these studies, a higher temperature led to multiple C-C bond cleavage, and decreased the SRO selectivity. The amount of fragments increased with increasing temperature at a fixed hydrogen pressure, and they attributed this change to the higher degree of the dehydrogenation of chemisorbed surface intermediate.

A similar conclusion was obtained by Arribas et al. (2002). Regardless of which Pt/USY catalyst was used, the selectivity to products with the same carbon numbers (C11) with the feed (1-methylnaphthalene) increased with decreasing temperature, although the relative concentration of isomers in the C11 fraction varied in the temperature range. They hypothesized that the increasing extent of secondary cracking and dealkylation reactions at higher temperature can account for this change. A similar trend was observed in another study about the ring opening of tetralin (Arribas et al., 2004). The yield of decalin decreased with increasing temperature, and the maximum amount of ROPs was reached at 300 °C. Beyond that point, the products with less than 10 carbon numbers increased due to consecutive dealkylation and cracking.

Albertazzi and co-workers (2003) studied a series of noble metals, including Rh, Pd, and Pt, supported on mesoporous MCM-41 catalysts. For Pd and Rh-containing catalysts, the activity decreased with increasing reaction temperature and the products distribution demonstrated different changes with temperature for catalysts.

Kubicka et al. (2004A) studied the ring opening of decalin over H-Beta-25, H-Beta-75, H-Y-12, H-Mordenite-20 and H-MCM-41, and noted that the conversion and yield of ROPs increased with the reaction temperature, but it was very easy for the ROPs to further react to produce cracking products. Jacquin et al. (2004) carried out a series of reactions of naphthalene over Pd/Pt bimetallic catalysts at different temperatures. Although the conversion increased with increasing temperature, the selectivity of ROPs decreased.

It should be noted that a low reaction temperature is not necessarily the best for SRO reactions. For example, Kubicka et al. (2004B) showed that increasing the reaction temperature favored the conversion of isomers into the ring opening products, as well as the successive cracking reactions. The yields of ring opening products depended on the extent of cracking reactions. Thus, an optimum temperature range exists to attain maximum yields of ROPs.

Hydrogen pressure is another critical parameter for SRO, as the variation of the hydrogen pressure can result in the change of product distribution. Teschner et al. (2000, 2003) found that the maximum rate of ring opening was reached at higher hydrogen pressure, and the turnover frequency (TOF), which was defined as the number of reacted MCP molecules per one surface Rh atom per hour, increased with hydrogen pressure. Arribas et al. (2002) observed that increasing H_2 pressure improved the yield of ROPs when other reaction parameters were unchanged; however, they also mentioned that the influence of pressure was limited over a range from 2.5 to 4.0 MPa at 300 °C and the influence would become insignificant beyond this range.

Kubicka et al. (2004B) found that the initial reaction rate for decalin ring opening did not change when they used argon to replace hydrogen. Consequently, they believed that the reaction for decalin was zero-order with respect to hydrogen.

Teschner et al. (2001) and Paal et al. (2005) reported that the overall MCP ring opening reaction on Rh catalysts had a positive reaction order with respect to hydrogen pressure. Zhuang et al. (1999) observed that MCP conversion reached a maximum with hydrogen pressure and dropped down beyond the point, and the optimum hydrogen pressure increased if the temperature increased.

In a recent review by Du et al. (2005), the impact of hydrogen pressure on selectivity and activity on different metal catalysts was reported. Even at temperature less than 300 °C, the activity of supported Pt catalysts increased with hydrogen partial pressure. After a maximum activity was reached, the activity began to decrease through a plateau range, which was related to the properties of support. Furthermore, the increase of hydrogen pressure favored the selectivity to the ring opening reaction.

2.2.4 Model Compounds

Methylcyclopentane (MCP) is the most extensively studied compound for the exploration of a ring opening catalyst. MCP can undergo various reactions, including cracking, ring enlargement, and ring opening. Alvarez et al. (1996) investigated the structural changes of Pt catalysts supported on non-acidic materials by analyzing the product distribution of methylcyclopentane.

Teschner et al. (2000 and 2003) studied MCP on different catalysts, including 5 % Rh/Al_2O_3, 5 % Rh/SiO_2 and 1 % Rh/Al_2O_3 and they concluded that the distribution of

ring opening products was related to the temperature and H_2 Pressure. Low temperature and high H_2 partial pressure favored the ring opening reaction.

Methylcyclohexane (MCH) is another commonly studied probe molecule. Figueras et al. (1997) used sulfated zirconia-supported platinum catalysts, and found the dominant reaction was the isomerization to alkylcyclopentane at low temperature (< 500 K) and toluene at temperatures higher than 550 K. The reaction followed the classical bifunctional mechanism.

McVicker et al. (2002) performed a thorough study on the ring opening of C_6-C_{10} mononaphthenes. Ir was recognized to be the most active metal for unsubstituted C-C bond opening in five-membered rings, but the activity decreased with the extent of alkyl substitution. However, the study of molecules containing two fused rings is not a common as single ring molecules due to their more complex structure and lower activity. Several studies have examined catalytic ring opening activity using decalin and tetralin as model compounds. Kubicka et al. (2004A and 2004B) investigated ring opening of decalin over zeolites, and they proposed a clear and convincing reaction mechanism for decalin ring opening and suggested that the reaction proceeded through several intermediates that were identified. Santkunaporn et al. (2004) reported that that Pt introduction into HY zeolite greatly enhanced the activity for catalyzing tetralin.

Arribas et al. (2002) studied the hydrogenation and ring opening of 1-methylnaphthalene and tetrahydronaphthalene over Pt/USY zeolite catalysts. They reported that the reaction was temperature dependent and secondary cracking and dealkylation reactions happened based on products distribution. Additionally, model

components of pyrolysis gasoline, i.e. aromatics with 6 to 9 carbon atoms, have also been investigated (Raichle et al., 2002).

2.3 Properties of ZrO_2-Based Catalysts

The combination of a Group VIII metal and a solid acid is generally considered to be an excellent catalyst for ring opening reactions. In this regard, ZrO_2-based catalysts have attracted more and more interest due to their excellent properties, high thermal stability, excellent acidity, and reducing and oxidizing ability. (Calafat et al., 2000; Bhaskar et al., 2001).

2.3.1 Structure of Zirconia

Pure zirconia (ZrO_2) has a high melting point (2700 °C), low thermal conductivity and provides chemical and corrosion inertness to temperatures above the melting point of alumina (http://www.accuratus.com/zirc.html). Zirconia exists in three crystal phases being monoclinic, tetragonal and cubic, and undergoes phase transformation with changes in preparation temperature. At temperatures greater than 2370 °C, zirconia has a cubic structure, at temperatures below 1170 °C it transforms to the monoclinic structure, and at temperatures in between it has a tetragonal structure (http://www.accuratus.com/zirc.html).

2.3.2 Stabilization of Zirconia

Pure zirconia is monoclinic at room temperature and changes to the tetragonal form at about 1000 °C. The transformation from tetragonal to monoclinic for ZrO_2 is rapid and is accompanied by a 3 to 5 percent volume increase that causes extensive cracking in the

material. Therefore, pure zirconia has low thermal shock resistivity (http://www.americanelements.com/newpage3.htm).

The incorporation of a second metal oxide can prevent this crystal structure transition, and several effective secondary oxides are MgO, CaO, and Y_2O_3 (http://www.accuratus.com/zirc.html), and a sufficient amount of secondary oxide can stabilize the tetragonal (and cubic) structure at room temperature. These stabilized tetragonal (and cubic) zirconias do not, in general, undergo phase transformation during heating and cooling (http://www.accuratus.com/zirc.html). When a secondary metal oxide is added to the pure zirconia, the structure will convert into a tetragonal phase at a temperature higher than 1000 °C. The mixture of a cubic phase and monoclinic or tetragonal phase can be stable at even lower temperatures. This is determined by the grain size, the sample thermal history, and the stabilizers (http://www.accuratus.com/zirc.html). There are two partially stabilized zirconias available commercially, TTZ (tetragonally toughened zirconia) that is stabilized by MgO and TZP (tetragonal zirconia polycrystal) that is stabilized by primarily yttria, and to a lesser extent ceria (http://www.americanelements.com/newpage3.htm). Usually, the fully stabilized zirconia forms a cubic solid solution when additional secondary oxides are added preventing a phase transformation from room temperature up to 2500 °C (http://www.americanelements.com/newpage3.htm).

2.3.3 Catalytic Activity of Zirconia Supported Catalysts

There are a limited number of studies that have been published regarding zirconia as a catalyst for fuel processing and reforming. For example, Maity et al. (1999) carried

out a detailed study of ZrO_2 supported hydrotreating catalysts. The HDS activity of MoS_2/ZrO_2 catalysts was higher than that of MoS_2/Al_2O_3 catalysts, while ZrO_2 catalysts gave less activity for hydrogenation (HYD). However, Hamon et al. (1991) obtained the opposite conclusion for HYD activity.

2.3.4 ZrO_2 as a Ring Opening Catalyst

2.3.4.1 Effect of Mo Incorporation

ZrO_2-MoO_3 has been studied as a support for different hydrotreating reactions due to its superior properties, particularly its acidic and basic properties, high thermal stability and surface area. Calafat et al. (2000) reported that the BET surface area of ZrO_2-MoO_3 increases to a maximum value with the introduction of Mo. They also found that the preparation procedure affected the properties of catalyst. For example, ZrO_2-MoO_3 prepared by late addition of Mo had higher surface area than those by co-precipitation methods, and they attributed this to the interaction between Mo and Zr. According to Maity et al. (2000), molybdenum oxide incorporation can lead to the crystal phase transformation of ZrO_2 from a monoclinic to tetrahedral structure. A similar observation has been made by Xie et al. (2000). Temperature programmed reduction (TPR) patterns suggested two different reduction regions for MoO_3, with an increase in reducibility with increasing Mo loading (Bhaskar et al., 2001). Another important conclusion from the same study was that low Mo loading resulted in high molybdenum oxide dispersion, which was related to the catalyst activity, as suggested by temperature programmed desorption (TPD) of NH_3. MoO_3 has also been suggested to enhance the sulfur-resistant ability of zirconia (Bhaskar et al., 2001).

Previous work done by Kenney (2004) also suggested that the introduction of MoO_3 stabilizes the tetragonal structure of zirconia. The monoclinic phase was dominant for catalysts with low Mo loading, and with increasing Mo content, the crystalline structure underwent a phase transition. At a loading of 4.7 at. % Mo, the tetragonal phase became the major phase and beyond that composition ZrO_2 existed in single tetragonal phase. It was hypothesized that molybdenum opposed the transition from tetragonal to monoclinic by keeping the zirconia grains size below a critical size. According to Kenney (2004), Mo incorporation not only stabilized the tetragonal crystalline structure, but also affected other catalytic properties, such as BET surface area, reducibility and acidity, and subsequently the activity for MCP conversion.

2.3.4.2 Effect of Iridium Incorporation

Iridium based catalysts have been studied for several significant reactions, including ring opening. Walter et al. (1995) studied the reaction of methylcyclohexane and reported that the ring opening of methycyclohexane can occur on Ir and Ru catalysts. Nylen et al. (2004) published the results of ring opening for indan, which is a compound with a benzene ring adjacent to a C5 naphthenic ring and has not been extensively studied. They catalyzed the ring opening of indan over Pt, Ir and Pt-Ir/boehmite catalysts, and their results suggest that iridium has a high hydrogenolysis activity. Cunha et al. (2002) studied the hydrogenation of benzene and toluene over $Ir/\gamma\text{-}Al_2O_3$, and they reported the turnover frequency (TOF) values of both reactions were closely related to the Ir particle size. In the particle size between 2.0 and 3.0 nm, the TOF values were almost constant. The TOF values decreased in the particle size below 2.0 nm due to the interaction

between Ir atoms and oxygen ions of alumina. In a recent study, Aboul-Gheit (2005) found that the combination of Ir and Pt supported on H-ZSM-5 had higher hydrogenation activity than that of each of these metals alone. In addition to the previous studies, it is widely recognized that iridium based catalysts are active for HDS and HDN. For example, Ir supported on ASA displayed a relatively high activity of HDS of diesel fuel at 623 K (Navarro et al., 1996), and an investigation of HDN of pyridine over Ir-alumina showed that Ir was highly active for HDN, even higher than Pt catalysts (Cinibulk et al., 1999).

McVicker et al. (2002) showed that Ir/Al_2O_3 had high activity and selectivity for cyclopentane and bicyclonaphthene ring opening. They observed that iridium-based catalysts are the most active and selective for breaking unsubsititued C-C bonds in five-membered ring compounds, compared to platinum, ruthenium, and rhodium based catalysts. However, the rate for ring opening was much slower for alkylcyclohexanes than for alkylcyclopentanes. In general, iridium has been considered as the most promising metal for ring opening in all cases.

2.4 Summary

The production of diesel fuel with a higher cetane number and ignition quality requires more active and selective catalysts. The combination of aromatic saturation and selective ring opening guarantees higher cetane number, and this reaction is favoured using a bifunctional catalyst with acidic and metallic sites. However, a significant research challenge is balancing the acidic and metallic functionalities to promote

selective ring opening and limit the extent of dealkylation and molecular weight reduction.

In this study, Ir/ZrO_2-MoO_3 was chosen as catalyst to study the selective ring opening of methylcyclopentane and cyclohexane. The combination of a metal and a solid acid is generally considered as the catalyst for ring opening, and the properties of Ir/ZrO_2-MoO_3 would appear to be ideal to promote selective ring opening.

CHAPTER 3

EXPERIMETAL METHODS

3.1 Catalyst Preparation

3.1.1 Chemicals

The chemicals used in this research are summarized in Table 3.1.

Table 3.1 List of Chemicals

	Molecular formula	Grade	Supplier	Remarks
Zirconyl chloride octahydrate	$ZrOCl_2.8H_2O$	98 % pure	Sigma-Aldrich	ZrO_2 precursor
Ammonium heptamolydate	$(NH_4)_6Mo_7O_{24}.4H_2O$	Certified A.C.S grade	Fisher Scientific	MoO_3 precursor
Ammonium hydroxide	NH_4OH	ACS reagent grade	Sigma-Aldrich	Adjust pH
Iridium atomic absorption standard solution	Ir in 10 wt % HCl	996 μg/ml	Sigma-Aldrich	Iridium precursor
Gamma Alumina Spheres	γ-Al_2O_3	AL 2700	Davison Catalysts	

3.1.2 Synthesis of ZrO_2-MoO_3

A series of ZrO_2-MoO_3 catalysts with different atomic concentrations of molybdenum (0, 0.01, 0.02, 0.03, 0.04, 0.05) were prepared via a co-precipitation method (Calafat et al., 2000). Using this method, $ZrOCl_2.8H_2O$ and $(NH_4)_6Mo_7O_{24}.4H_2O$ were weighed and added to a beaker. The resulting solution was heated on a hotplate with continuous stirring, and the temperature maintained at approximately 95 °C. When the solids were thoroughly dissolved, ammonium hydroxide was added slowly to precipitate the metal oxide, and the pH was monitored using a pH meter. During precipitation, the viscosity of the solution increased and the stirring speed had to be modified correspondingly so that the solution was well mixed. When the pH reached 9.25, the solution was vacuum filtered and then it was washed with distilled water several times. The filter cake was collected in a crucible and placed in the fume hood overnight to dry. The metal oxide was subsequently dried at 140 °C for eight hours, and then the sample was calcined in a furnace at 500 °C for two hours. The samples were slowly ground into fine powders in a well-cleaned mortar and put into vials for future use.

The samples prepared and the corresponding amounts of each precursor are listed in Table 3.2. It should be noted that some experimental results in the following chapters are based on the samples made previously by Kenney (2004), who prepared the samples with Mo atomic concentration at 0 %, 3 %, 5 %, 9 %, 11 %, 16 % and 19 %. These data are included for additional comparison to the samples prepared in the present study.

Table 3.2 Sample list with different Mo atomic concentration

Sample#	Mo	Mol_{Zr}	$ZrOCl_2.8H_2O$(g)	Mol_{Mo}	$(NH_4)_6Mo_7O_{24}.4H_2O$(g)
B0	0 %	0.125187	40.3477	0	0
B1	1 %	0.094193	30.3584	0.00094	0.1660
B2	2 %	0.094185	30.3557	0.001893	0.3343
B3	3 %	0.094206	30.3626	0.002831	0.4999
B4	4 %	0.094197	30.3597	0.003769	0.6654
B5	5 %	0.094184	30.3554	0.004711	0.8318

3.1.3 Iridium Impregnation

Iridium was incorporated into the ZrO_2-MoO_3 via wet impregnation using iridium in 10 wt % HCl (996 μg/ml). Under continuous stirring using a glass rod, the iridium precursor solution was gradually added into pre-weighed ZrO_2-MoO_3 using a micropipette until the solids were slightly oversaturated by the precursor. The samples were then placed in a fume hood for about 3 hours, dried in the oven at 120 °C overnight, and calcined at 500 °C for 4 hours.

Iridium was also incorporated into γ-Al_2O_3 as a comparison using the same procedure as previously discussed. Two series of catalysts with different iridium loadings, including 30 and 300 ppmw were prepared for each catalyst to determine the effect of Ir loading on catalytic activity and selectivity. In order to ensure metal was well dispersed, the iridium precursor was diluted with 10 parts distilled water before impregnation for 30 ppmw samples.

3.2 Catalyst Characterization

Several catalyst characterization techniques were used in this research, including x-ray photoelectron spectroscopy (XPS), x-ray diffraction (XRD), instrumental neutron activation analysis (INAA), and temperature programmed techniques. The general theory and experimental parameters used in each technique are summarized in the following sections.

3.2.1 X-Ray Photoelectron Spectroscopy (XPS)

X-ray photoelectron spectroscopy (XPS) is an analysis technique used to obtain chemical information about the surfaces of solid materials. Both the composition and the chemical state of surface constituents can be determined by XPS.

During the analysis a sample is loaded in an ultra high vacuum chamber, which is typically lower than 10^{-9} Torr, and is bombarded with a low-energy x-ray source of either Mg Kα (1253.6 eV) or monochromatic Al Kα (1486.6 eV) x-rays. Electrons are emitted due to the photoelectric effect. The mean free path for photoelectrons ranges from about 5 to 100 Å. The kinetic energy of a photoemitted core-level electron is a function of its binding energy and is one of the characteristics of the element from which it was emitted. The energy balance equation for the process is given by Equation 3.1;

$$E_{binding} = E_{photon} - E_{kinetic} - \Phi \qquad (3.1)$$

where the energy of photon, E_{photon}, is a known quantity for the specific x-rays and Φ is the spectrometer work function, which is a small constant value. Therefore, the binding

energy of the ejected electron can then be determined from Equation 3.1. The binding energy is a relative value, and can be defined as the energy difference between the initial and final states of the photoelectrons.

Because the binding energy of emitted electrons is very specific and unique for the element that the atom belongs to, the spectrum gives information on the elemental composition in the surface region. Moreover, the chemical potential and polarization of compounds can lead to the chemical shifts in the elemental binding energy, which can be used to determine the chemical state of the analyzed compounds.

The photoelectrons emitted from a sample are detected by an electron energy analyzer, and their energy is determined as a function of their velocity entering the detector. By counting the number of photoelectrons as a function of their energy, a spectrum representing the surface composition is obtained. The area under a peak in the spectrum is a measure of the relative amount of the element represented by that peak. In order to calculate the relative composition, Equation 3.2 was used;

$$C_E(\%) = \frac{I_i / RSF_i}{\sum I_i / RSF_i} 100\% \qquad (3.2)$$

where $C_E(\%)$ is the percent elemental composition, I_i is the intensity corresponding to the area under the peak in XPS, and RSF_i is relative sensitivity factor. The RSF values for Zr and Mo are 2.576 and 3.321, respectively. The peaks were identified according to their binding energies.

In this study, XPS studies were carried out on Axis HSi 165 XPS system with monochromatic Al Kα X-ray (1486.6 eV). Before analysis, about 50 to 100 mg fine

sample powders were evenly dispersed to form a very thin layer in the copper sample cup. The samples were degassed under a pressure of about 5×10^{-9} Torr for about 30 minutes. Survey spectra were obtained from 0 to 1100 eV with a pass energy of 160 eV, a dwell time of 0.1 sec and a step size of 0.3 eV. For high-resolution scans, the pass energy was 20 eV, dwell time was 0.2 sec, and the step size was 0.1 eV. The sweep times were determined based on optimizing the signal-to–noise ratio.

3.2.2 Instrument Neutron Activation Analysis (INAA)

Atomic absorption spectroscopy (AAS) and inductively coupled plasma-atomic emission spectroscopy (ICP-AES) are the most commonly employed methods to determine the trace elemental concentration. However, both methods require that the analyzed compounds be completely dissolved, and it is usually very difficult to dissolve some metal oxides. Instrumental neutron activation analysis (INAA) has a significant advantage in this respect. INAA is a nondestructive process of determining the chemical composition of a sample, as the sample is not changed in any manner by chemical manipulation or the introduction of any material prior to irradiation. INAA measures the total amount of an element in a material without regard to chemical or physical form. Samples analyzed can be liquids, solids, suspensions, slurries, or gases and do not have to be put in a solution or vaporized.

INAA is a very sensitive analytical technique for both qualitative and quantitative analysis of trace elements in samples. For many elements and applications, INAA can even offer sensitivities of the order of parts per million. INAA is generally used as the

"referee method" of choice when disagreement exists about the results from other methods due to its accuracy and reliability.

Figure 3.1 shows the basic principle and process of INAA. In an INAA experiment, the stable target nucleus in the sample becomes radioactive by capturing a neutron in a flux of incident neutrons. The produced radioactive nucleus in this activation process will decay by emitting a beta particle and delayed gamma ray, which has a unique half-life. A high-resolution gamma-ray detector is used to analyze these "delayed" gamma rays (http://www.missouri.edu/~murrwww/pages/ac_naa2.shtml).

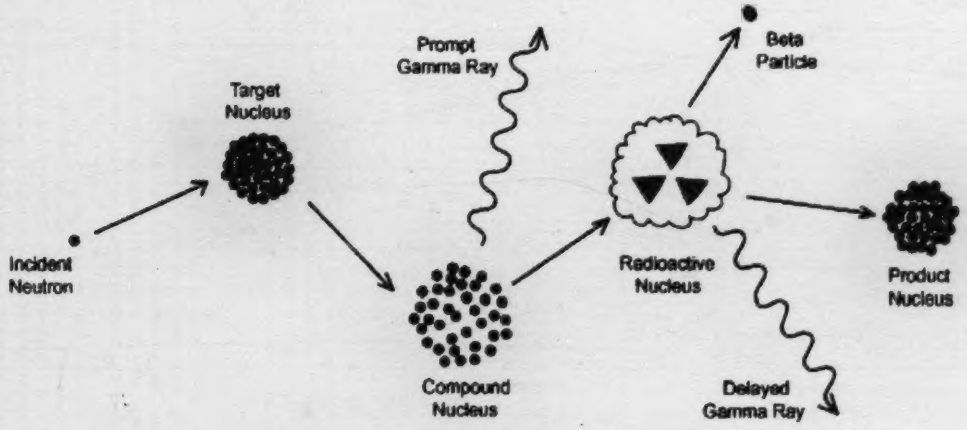

Fig 3.1. General Principle of INAA.

(Reprinted from http://www.missouri.edu/~murrwww/pages/ac_naa2.shtml)

The measured count rate (R) of the gamma rays from the decay of a specific isotope in the irradiated sample can be related to the amount (n) of the original, stable isotope in the sample through Equation 3.3;

$$R = \epsilon I_\gamma A = \epsilon I_\gamma n \phi \sigma (1-e^{-\lambda t_i}) e^{-\lambda t_d} \qquad (3.3)$$

where R is measured gamma-ray count rate (cps), A is absolute activity of isotope ^{A+1}Z in sample, ϵ is absolute detector efficiency, I_γ is absolute gamma-ray abundance, n is number of atoms of isotope ^{A}Z in sample, ϕ is neutron flux (neutrons·cm^{-2}·sec^{-1}), σ is neutron capture cross section (cm^{2}) for isotope ^{A}Z, λ is radioactive decay constant (s^{-1}) for isotope ^{A+1}Z, t_i is irradiation time (s), and t_d is decay time (s). The energies of the delayed gamma rays are used to determine which elements are present in the sample, and the number of gamma rays of a specific energy is used to decide the amount of an element in the sample (http://www.missouri.edu/~murrwww/pages/ac_naa2.shtml).

In this study, INAA was used to determine the iridium concentration in the series of samples. About 100 mg of sample was placed into a plastic sample holder. Analysis was carried out in SLOWPOKE II produced by AECL (Atomic Energy of Canada Limited). The relative abundance of iridium isotopes ^{191}Ir and ^{193}Ir are 37.3 % and 62.7 %, respectively. The main reactions in this analysis are;

$$^{191}_{77}Ir + ^{1}_{0}N \Rightarrow ^{192}_{77}Ir$$

$$^{193}_{77}Ir + ^{1}_{0}N \Rightarrow ^{194}_{77}Ir$$

The emitted delayed gamma rays were detected by 22 % hypepwe Ge detector. The characteristic gamma rays for ^{192}Ir are 316.5, 308.4, 295.9 and 468.1 keV, while those rays for ^{194}Ir are 328.45 and 293.5 keV. In present study, a delayed gamma ray at 328.45 KeV of ^{194}Ir was used for analysis because of much shorter half life of ^{194}Ir (19.28 hours) compared to ^{192}Ir (73.831 days).

3.2.3 X-Ray Diffraction

X-ray Diffraction (XRD) is a widely used analytical technique to identify and characterize crystalline materials. Monochromatic x-rays are used to determine the inter-planar spacing, and samples are analyzed as powders in random. When Bragg's law for constructive interference is met, a "reflection" happens following Equation 3.4;

$$n\lambda = 2d\sin\theta \tag{3.4}$$

where θ is the angle between the atomic planes and the incident x-ray beam, n is an integer, λ is the wavelength of the incident x-ray source, and d is the lattice spacing between the planes in the crystal. Analysis of the position of the diffraction effect leads to knowledge of the size, shape, and orientation of the unit cell.

High resolution x-ray diffraction (HRXRD) systems are used in the situation where desired diffraction peaks are too close each other to resolve using broad spectrum radiation. A natural crystal like Si (1 1 1) is utilized to increase resolution by filtering the beam to a much narrower band. HRXRD has comprehensive applications and can describe crystal orientation, layer thickness in crystalline layer, roughness, lattice mismatch, and chemical composition of material (http://www.panalytical.com/index.cfm?pid=147).

The XRD measurements used in this study were carried out on the SUNY beamline X3B1 at the National Synchrotron Light Source (NSLS), Brookhaven National Laboratory (BNL). A double Si (1 1 1) crystal monochromator at a wavelength of 0.69952 Å was used to generate the synchrotron beam. The monochromator was

calculated by seven reflections using a NIST corundum X-ray diffraction standard (NIST 1976a). The diffracted beam was analyzed with a Ge (1 1 1). X-ray scattering patterns were obtained at a step of 0.01° from 5° to 55° at room temperature (Kenney et al., 2005).

3.2.4 Temperature Programmed Techniques

Temperature-programmed techniques were introduced in the 1950's as an important method for analysis in many areas of industry and research. A good understanding of surface structure and surface chemistry of catalysts is critical to design and develop catalysts with superior properties. There are several temperature programmed techniques for studying surface reactions and molecular adsorption on a surface. These kinds of techniques are appropriate for the study of highly temperature dependent phenomena, such as adsorption, desorption, oxidation, and other chemical reactions. All of these applications can be used on a qualitative and quantitative basis.

These applications are usually achieved using a programmed heating system in a linear manner. In this study, all of these operations were performed on automated chemisorption system (AutoChem II 2920, Micromeritics). The simplified steps in the system can be described as follows; gas flows into the system, the gas interacts with the sample, as the temperature changes in the sample tube the detector collects the data when the resulted gas flows through it, and finally the data is processed and analyzed on the control module (Operation manual of AutoChem II 2920, 2003).

3.2.4.1 Introduction to the AutoChem II 2920

The AutoChem II 2920 system is an automated chemisorption analyzer designed and developed by Micromeritics. Figure 3.2 shows the Autochem II 2920 with the cold trap, furnace and vapor generator. The unit has a programmable furnace and is interfaced to a computer with data acquisition software, so that the analysis results can be recorded and analyzed.

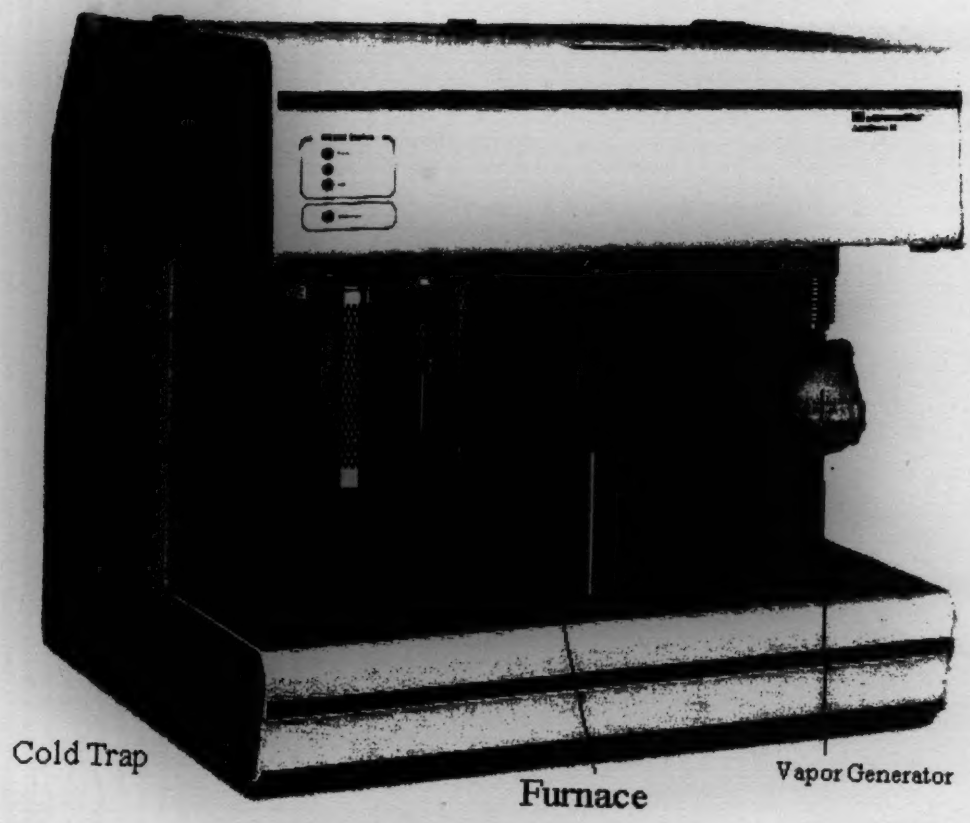

Fig. 3.2 AutoChem II 2920

3.2.4.2 Temperature Programmed Reduction (TPR)

When a catalyst contains reducible metal oxides, temperature programmed reduction (TPR) can be used to determine the number of reducible species and temperature where reduction occurs. Some catalysts demonstrate activity only at reduced state. Therefore, in-situ reduction is necessary to obtain an effective catalytic reaction sometimes.

The TPR analysis is performed by flowing a reducing gas (generally hydrogen in an inert carrier gas) through the sample. While the gas mixture is passing over a catalyst, the temperature of the sample is increased linearly with time and the consumption of hydrogen is monitored. Changes in the concentration of the exhaust gas are detected by a thermal conductivity detector (TCD) and analyzed. When reduction is complete, no additional hydrogen is consumed and the thermal conductivity of gas mixture does not change. The volume of hydrogen uptake is obtained after calibration. A couple of reduction peaks will be observed during the heating process if there is more than one type of reducible site in the catalysts. The strength and concentration of different reducible sites can be determined from the area and position of the peaks.

In this study, approximately 120 mg of catalyst was used for each TPR experiment. TPR analysis was performed using a reducing gas of 10 % H_2 in argon flowing at 50 ml/min. The catalysts were heated from ambient temperature to 500 ^{o}C at a ramp rate of 10 ^{o}C/min, and the catalyst was held at 500 ^{o}C for 1 hour. Then the gas was switched to helium at a flowrate of 50 ml/min and temperature returned to ambient condition.

3.2.4.3 NH_3 Temperature Programmed Desorption (TPD)

Temperature programmed desorption (TPD) analysis can be used to determine the number, type and strength of acidic sites on the solid surface. TPD consists of heating a sample at a constant rate and measuring the quantity of material desorbed with temperature. When the heat is high enough to overcome the activation energy with rising temperature, the bond between the adsorbate and adsorbent breaks and desorption will occur. Desorbed signals at different temperatures will be observed if several types of active sites are present in the sample.

TPD of ammonia is a commonly used method for characterizing the site densities in solid acids. Ammonia is such a strong basic molecule that it can titrate even very weak acid sites. Furthermore, the small size of ammonia allows it to access to all the pores with different sizes into the solid acid.

In this study, TPD of ammonia was performed to obtain the detailed information about acidity of Ir/ZrO_2-MoO_3 catalysts. Ammonia desorption was carried out using the following procedure. About 150 mg sample was added into the quartz sample tube, and the sample was degassed by flowing the helium at a flowrate of 20 ml/min. The temperature of sample was heated up from ambient temperature to 500 °C in order to remove any adsorbed species from the surface of catalyst. The temperature was reduced to 80 °C, and the gas was switched from helium to 15 % NH_3 in helium and ammonia was allowed to continuously chemisorb for 30 minutes. Subsequently, the remaining ammonia molecules were flushed out with helium at a flowrate of 25 ml/min and the flow of helium was maintained while the temperature was increased to 500 °C at the rate of 20 °C/min.

The ammonia concentration in the effluent stream was measured with the thermal conductivity detector and the total amount of desorbed ammonia was determined by using the software in Autochem II 2920 after TPD calibration. The trace data was exported into Excel and edited in peak fitting software. The peaks were fitted and the areas under different peaks were integrated, whereby each peak represents a type of acid site. The desorbed ammonia was assigned to an acid site based on the area under the peak because the area is proportional to the amount of desorbed ammonia.

If the assumptions that no readsorption of gas takes place and when the molecules are adsorbed on a homogeneous surface without mutual interaction prevail, the following equation applies (AutoChem II 2920 Manual, 2003);

$$\ln\left(\frac{\beta}{T_m^2}\right) = -\frac{H_d}{RT_m} + \ln\left(\frac{H_d A}{RC}\right) \qquad (3.5)$$

where β is ramp rate in °C/min, T_m is temperature at peak max, R is the gas constant, A is the quantity adsorbed at saturation, C is a constant related to the desorption rate, and H_d is heat of desorption in J/mole. The slope can be determined by plotting $2lnT_m - ln\ \beta$ *vs.* $1/T_m$, and then the following equation is obtained;

$$H_d = s\ x\ R \qquad (3.6)$$

In order to calculate heat of desorption, the procedure of ammonia adsorption and desorption is repeated at different temperature ramping rates ranging from 25 °C to 45 °C because at least two points are required in order to obtain the energy of desorption.

Analysis data is plotted as desorbed quantity versus temperature. The desorbed quantity at specific temperature demonstrates the number of active sites.

3.2.4.4 CO Chemisorption

CO chemisorption can provide information about metal dispersion and active particle size about iridium on Ir/ZrO_2-MoO_3 catalysts. Metal dispersion is defined as the ratio of active atoms exposed to the gas phase to total number of potentially active atoms incorporated into the catalyst, which can be determined by bulk chemical analysis. Chemisorption analysis described here is used to determine the available active metals for reaction based on the following equation;

$$D = (N_s/N_t)\times 100\% = \frac{AU}{\nu W}\times 100\% \qquad (3.7)$$

where A is atomic weight (g/atom), U is amount of gas consumed (moles/gram of catalyst), ν is stochiometry of reaction, and W is weight fraction of metal in the catalyst. Active particle size can also be obtained from this type of analysis. The calculation of active particle size is based on the assumption that the crystallite shape is a type of regular geometry, where a sphere is widely used as the geometry. It is noted that the calculated particle size, such as diameter, is average diameter of active metals which adsorption occurs at.

CO chemisorption was performed in a similar manner as the ammonia TPD analysis, with the key difference that the sample was exposed to 10 % CO in helium using the injection loop. When the saturation was reached, the injected gas volume did

not change for each time. The adsorbed amount was the difference between the total injected amount and the unbonded amount.

The experimental procedure can be described as follows. A flow of 10 % H_2 in argon at 50 ml/min was used as reducing gas. After TPR analysis, the temperature was reduced to 50 °C and held for 10 minutes until the TCD baseline was stable. Then, 10 % CO in helium was switched as a loop gas. 1.5 waiting minutes were set up between injections. The sample was dosed several times (e.g. 8 doses) until the resulted peaks were equal in area.

3.2.4.4 BET Surface Area

The surface areas of the catalysts were measured by using BET method. In a typical BET experiment, a mixture of N_2 and He is used as the analysis gas. By passing the mixed gas with different nitrogen concentration over the samples that are cooled by liquid nitrogen, the surface area can be determined by calculating the amount of desorbed nitrogen and equations (3.8), (3.9), and (3.10) (Operation manual of AutoChem II 2920, 2003).

$$SA = \frac{V_m}{22414} \times (6.023 \times 10^{23}) \times A_{N_2} \tag{3.8}$$

$$V_{STP} = \frac{V_a}{SW} \times \left(\frac{273.15K}{273.15K + T_a} \right) \times \left(\frac{P_a}{760mmHg} \right) \tag{3.9}$$

$$V_m = V_{STP}\left(1 - \frac{P}{P_a}\right) \tag{3.10}$$

where *SA* is the surface area in m^2/g, V_m is the volume of monolayer in mL, A_m is the surface area of N_2 molecule, V_{STP} is the volume sorbed in mL/g of sample at standard temperature and pressure, V_a is the volume sorbed at ambient conditions in mL, *DW* is the sample mass in g, *P* is absolute pressure of N_2 (estimated by %N_2/100 x P) in mmHg, P_a is ambient pressure in mmHg, and P_0 is saturation pressure of N_2 (estimated by P_a + 15 mmHg) in mmHg.

In this study, a 3-point BET method was employed. Prior to BET measurement, the catalyst was pretreated by passing high purity helium at a flowrate of 50 ml/min and heated up to 300 ℃. The purpose of pretreatment was to remove adsorbed species from the surface of catalysts that may influence the adsorption uptakes. After the pretreatment, the catalyst was cooled using liquid nitrogen. The analysis gas was then switched to 30 % N_2 in He. The catalyst in U-shaped quart tube was immersed in a Dewar full of liquid nitrogen and some nitrogen was adsorbed on the surface of catalyst. When the adsorption was finished, another Dewar full of water was used and nitrogen on the surface was desorbed. The gas concentration in the effluent stream was monitored with the thermal conductivity detector and the area under desorption peak was integrated using the software installed in AutoChem II 2920. The same procedure was repeated except that the analysis gas was changed to 20 % N_2/He and 10 % N_2/He, and 3 points were obtained.

3.3 Catalytic Reaction

Two different reaction modes were used in this study. One was a pulse mode, which was carried out in AutoChem II 2920 as an initial proof-of-concept study. The resultant exhaust was analyzed in Dycor M200ED mass spectrometer. The other was a reaction that was performed in a batch reactor heated by sand bath. The resulting liquid products were separated in gas chromatography firstly, and then flowed into the mass spectrometer for identification and quantification.

3.3.1 Chemicals

The main chemicals used in the study are as followings:

- Methylcyclopentane: 97 % from Sigma-Aldrich (reactant)
- Cyclohexane: ≥99.7 % HPLC grade from Sigma Aldrich (reactant)
- Hexadecane: ≥99 % from Sigma Aldrich (solvent)

3.3.2 Pulse Mode

The AutoChem II 2920 was used as a pulse mode reactor for initial proof-of-concept studies using methylcyclopentane (MCP). The reaction was performed at 300 °C and 100 kPa. About 35 ml of MCP was filled in an Erlenmeyer flask, and the flask was connected with vapor generator and surrounded by vapor generator heating mantle. An aerator was immersed into MCP.

Before reaction, the catalyst was degassed under helium at 500 °C and then it was cooled down to room temperature. The carrier gas was switched to 10 % H_2 in argon and the sample was heated to 500 °C and held for 1 hour. After reduction, the temperature

was decreased to 300 °C. The MCP was vaporized at a reflux temperature of 45 °C and then filled the sample loop with approximately 10 ml with 10 % H_2/Ar. After about 30 minutes, the MCP vapor was injected into the carrier gas via a valve change from fill to inject status, allowing 10 minutes for vapor to pass through the catalyst. Then the valve was switched back and the loop was refilled until next injection.

The Dycor Quadrupole Gas Analyzer was used to monitor the exhaust gas composition. The mass to charge ratio from 1 to 88 was scanned and recorded every six seconds. According to a reference mass spectrum for methylcyclopentane (http://webbook.nist.gov/cgi/cbook.cgi?Name=methylcyclopentane&Units=SI&cMS=on) , MCP has fragments with fairly strong intensity at mass to charge (m/z) ratios of 41, 56 and 69. In this study, the experiments with and without catalysts were performed, respectively, and the conversion of MCP for different catalysts was calculated based on the intensity change of the m/z = 41.

3.3.3 Reaction in Batch Reactor

Following the initial proof-of-concept studies using methylcyclopentane, the conversion of cyclohexane was studied in a high-pressure batch reactor. A reactant solution was prepared by diluting 10 g cyclohexane in 60 g hexadecane. The cyclohexane ring opening study was carried out in a 15 ml stainless steel batch reactor, and the reactor was heated by a fluidized sand bath. The catalysts were first reduced in a hydrogen environment for two hours at 500 °C and 1.8 MPa H_2 pressure, and the reaction was performed for eight hours under 400 °C and 7 MPa H_2 pressure. The liquid products were collected and analyzed by GC/MS.

3.3.3.1 Procedure

The microbatch reactor (made by machine shop in Chemical and Materials Engineering Department) was weighed, and about 120 mg catalyst was weighed and added into the reactor. The reactor was pressurized with H_2 to about 700 kPa and leak-testing was performed after pressurizing. The reactor was placed and completely immersed in the pre-heated sand bath (500 °C) for two hours. During the course of reduction, the reactor was shaken up and down to minimizie the temperature gradient. When reduction had finished, the reactor was cooled down in air. The reactor was opened in a nitrogen glove box to prevent re-oxidation, and about 5 ml of the reactant mixture was added. Figure 3.4 shows the set-up used for the batch reactor experiments.

Fig 3.3 Experiment Setup in Sand Bath

The reactor was then pressurized with H_2 to achieve a final hydrogen pressure of 7 MPa, and the reactor was put into the sand bath at 400 °C for 8 hours. After the reaction was completed, the reactor was immediately quenched and the pressure was released and the weight of reactor, spent catalyst and products was measured. The liquid products were collected, and the reactor was thoroughly cleaned, dried up and weighed.

3.3.3.2 Products Analysis

Products from the reaction were analyzed by gas chromatography and mass spectrometry. The two analytical methods are used together for the identification of complex volatile materials. GC effectively separates the different constituents of the sample for subsequent analysis and identification by mass spectrometry (MS). The chromatographic separation relies on the interaction of the sample with a mobile phase and a stationary phase within the GC column. The sample is carried through the column by the mobile phase. The affinity of a particular molecule with the stationary phase determines the retention time of that constituent in the column. The molecules for each component of the sample will travel through the column at nearly the same rate and exit from the column within a narrow time band that is specific to that component. Thus, compounds with different retention times in the column are physically separated.

The typical GC capillary column consists of a small diameter tube with a thin film of a high-molecular weight polymer coated on the inside. The polymer is the stationary phase for the chromatographic process. The mobile phase can be any inert gas, but is typically helium. The instrument also includes a heated injection port to vaporize all

volatile constituents of the sample and an oven to keep the constituents in gas form as they pass through the column.

When a sample constituent elutes from the GC column, it enters the ionization chamber of the mass spectrometer where the molecules are ionized, which results in the loss of an electron from the molecule, and a positive ion is formed. Some of the molecular ions are further fragmented into additional ions and neutral fragments. The positive ions are then repelled out of the ionization chamber by a small positive charge within the chamber. Negative ions are also formed by the electron impact, but are not analyzed. The positive ions are separated according to their mass by a mass analyzer. The mass analyzer most commonly used in GC/MS is the quadrapole filter, in which the ions pass by four hyperbolic poles created by a radio frequency field. The poles separate the ions by their mass/charge ratio, successively focusing ions with increasing mass onto a detector for counting. The analyzer scans step-wise through a set range of mass values to evaluate the relative abundance of ions at each mass value. The quadrapole filter can perform a complete mass scan within the duration of a single GC elution band.

The instrument used in the analysis is a HP 5890 GC equipped with 5970 MSD and an automatic liquid sampler. The column is HP-5MS, whose dimension is 30 m in length, 0.25 mm diameter and 0.25 μm film thickness. The injection volume for each analysis was 1 μl with a split ratio of 50:1. The temperature of the injector and detector was maintained at 325 °C and 300 °C, respectively. The oven temperature was held at 50 °C for 5 minutes, increased to 300 °C at a ramp rate of 10 °C/min, and kept for 5 minutes. The total analysis time was about 35 minutes.

CHAPTER 4

RESULTS

4.1 X-Ray Photoelectron Spectroscopy

XPS was used to determine the actual Mo loading and oxidation state of the metals, which has been reported to be a crucial factor to affect the properties of catalysts (Calafat et al., 2000; Maity et al., 2000; Xie et al., 2000; Bhaskar et al., 2001). Figure 4.1 shows the survey scan spectrum for the catalyst with 1 at. % Mo. In a survey scan, energy peaks identify the elemental composition of the uppermost region of the analyzed surface. The elements, C, O, Mo and Zr were identified in current study. A similar spectrum with different relative intensities was obtained for all the other catalysts.

In addition to qualitative analysis, XPS can probe the elemental concentration and chemical state the surface region, and high-resolution multiple scans of major elements were obtained for this purpose. In this study, the atomic loading of Mo was a very important parameter to affect the properties of catalysts. Figure 4.2 shows the core levels of Zr 3d and Mo 3d for the catalyst with 1 at. % Mo. Each spectrum was deconvoluted into two peaks by using CASA software. The Zr 3d core level spectrum shows a Zr $3d_{3/2}$ and a Zr $3d_{5/2}$ peak at 183.2 eV and 180.8 eV, respectively, while Mo 3d shows a Mo $3d_{3/2}$ and a Mo $3d_{5/2}$ peak at 234.1 eV and 231.0 eV. The binding energies for the different elements in all catalysts are listed in Table 4.1. The reference binding energy was obtained from XPS handbook (1992) and NIST XPS database (http://srdata.nist.gov/xps/Bind_E.asp). The standard position for carbon is 285.0 eV, but the observed carbon position for all catalysts slightly shifted to lower binding energy,

which resulted in the binding energy shift for all the other elements. Thus, the binding energy for other elements was adjusted by considering the shift of carbon position, and the corrected binding energy is given in the last column. The binding energy of Mo and Zr showed very similar values for various samples. According to the binding energies of Zr and Mo, the composition can be assigned to ZrO_2 and MoO_3.

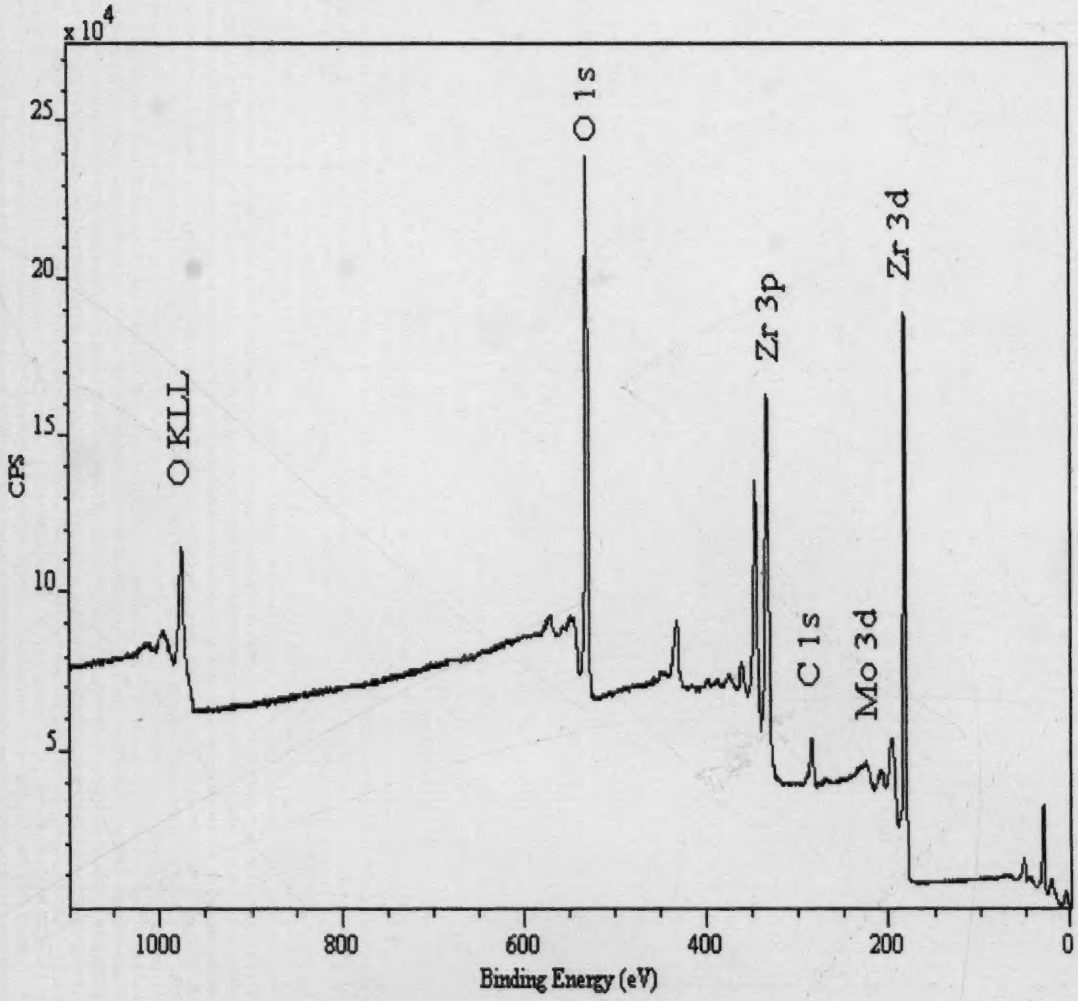

Fig. 4.1 XPS Survey Scan for catalyst with 1 at. % Mo

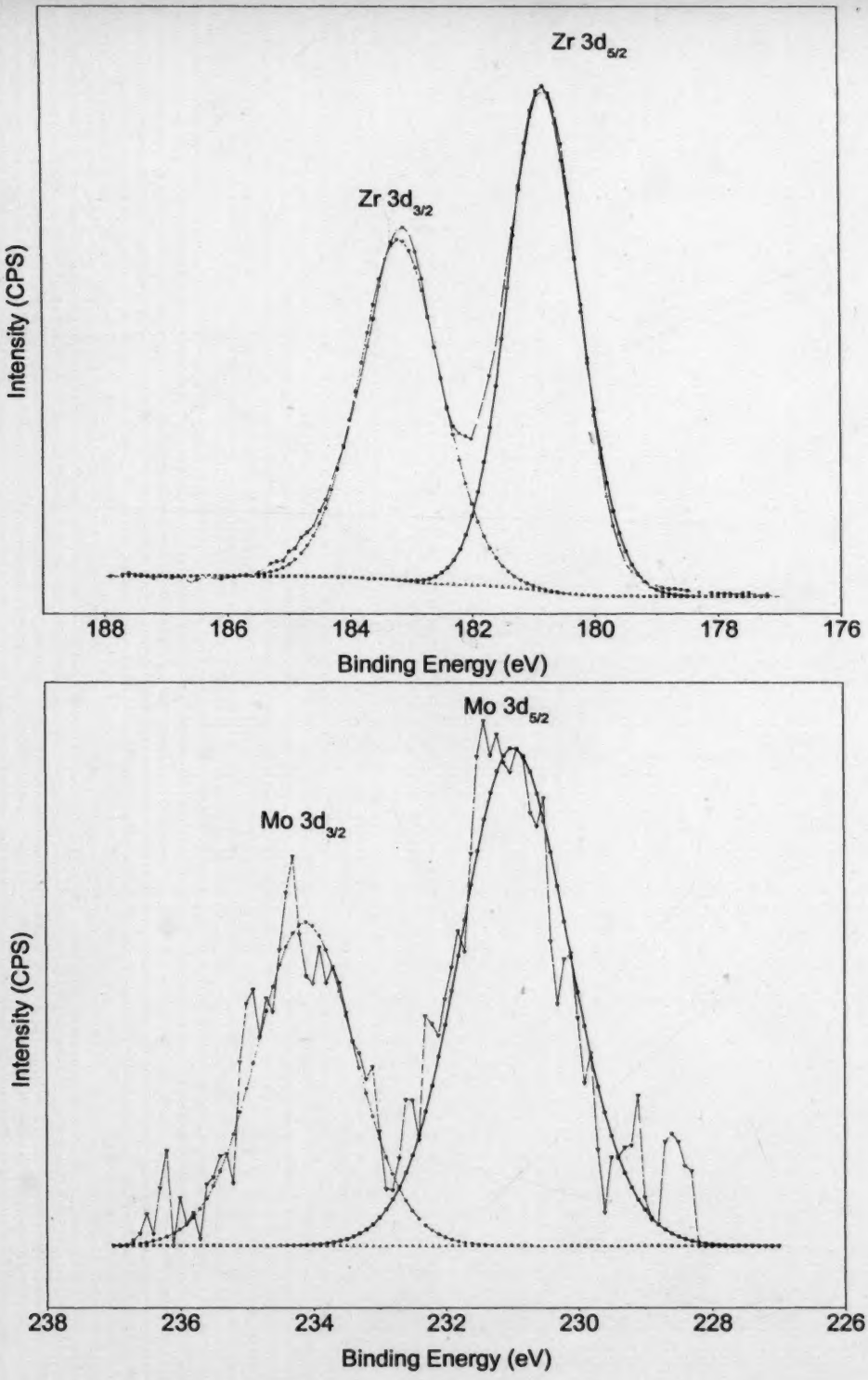

Fig. 4.2 XPS High Resolution Scan for catalyst with 1 at. % Mo

Table 4.1 XPS results of Ir/ZrO_2-MoO_3 catalysts

Theoretical Mo atomic loading	Atomic Concentration (%)	Actual Mo atomic loading	Peak	Binding Energy (eV)	Corrected Binding Energy (eV)[a]
1 %	56.6	0.7 %	O 1s	529.2	530.4
	18.2		C 1s	283.8	285.0
	25.0		**Zr $3d_{5/2}$**	**180.8**	**182.0**
			Zr $3d_{3/2}$	183.2	184.4
	0.2		**Mo $3d_{5/2}$**	**231.0**	**232.2**
			Mo $3d_{3/2}$	234.1	235.3
2 %	47.0	3.5 %	O 1s	529.2	530.5
	30.9		C 1s	283.7	285.0
	21.3		**Zr $3d_{5/2}$**	**180.8**	**182.1**
			Zr $3d_{3/2}$	183.1	184.4
	0.7		**Mo $3d_{5/2}$**	**231.0**	**232.3**
			Mo $3d_{3/2}$	234.1	235.4
3 %	54.8	4.7 %	O 1s	529.2	530.2
	19.9		C 1s	284.0	285.0
	24.1		**Zr $3d_{5/2}$**	**181.0**	**182.0**
			Zr $3d_{3/2}$	183.3	184.3
	1.1		**Mo $3d_{5/2}$**	**231.3**	**232.3**
			Mo $3d_{3/2}$	234.6	235.6
4 %	47.8	5.0 %	O 1s	529.5	530.5
	30.9		C 1s	284.0	285.0
	20.4		**Zr $3d_{5/2}$**	**181.2**	**182.2**
			Zr $3d_{3/2}$	183.5	184.5
	1.0		**Mo $3d_{5/2}$**	**231.4**	**232.4**
			Mo $3d_{3/2}$	234.5	235.5
5 %	47.8	6.7 %	O 1s	529.2	530.5
	33.4		C 1s	283.8	285.0
	17.5		**Zr $3d_{5/2}$**	**180.9**	**182.2**
			Zr $3d_{3/2}$	183.3	184.6
	1.2		**Mo $3d_{5/2}$**	**231.2**	**232.5**
			Mo $3d_{3/2}$	234.3	235.6

[a]Corrected binding energy is determined by considering the same BE shift of Carbon.

4.2 Instrument Neutron Activation Analysis (INAA)

Ir was not detected in XPS analysis in the present study due to the low level of iridium loading, therefore, INAA was used to determine the iridium concentration in samples. The initial iridium concentration results based on both ^{192}Ir and ^{194}Ir for catalysts with 300 ppmw iridium are in good agreement with each other and the expected iridium loadings. Therefore, iridium concentration for other catalysts was determined only by measuring the intensity of delayed gamma ray of ^{194}Ir at 328.45 keV. For catalysts containing about 30 ppmw Ir, higher neutron fluxes and longer irradiation times were used to increase the sensitivity. The standard iridium solution is 10 μg Ir/ml in HCl. Table 4.2 lists the iridium concentration for all the catalysts in the study. When the predicted and experimental results were compared, it was noticed that only a slight difference between them was found, which implies that the wet impregnation method was very reliable to incorporate the metal into the support material.

Table 4.2 Iridium concentration determined by INAA technique

Mo loading (at. %)	Theoretical Ir (μg/g)	Actual Ir (μg/g)	Uncertainty (± 1σ)
0 %	300	349	5
0.7 %	300	247	4
3.5 %	300	409	7
4.7 %	300	340	5
5 %	300	325	5
6.7 %	300	336	5
0 %	30	32.3	0.7
0.7 %	30	38.2	0.7
3.5 %	30	34.5	0.8
4.7 %	30	32.7	0.7
5 %	30	31.5	0.7
6.7 %	30	41.8	0.7
Ir/γ-Alumina	300	332	5
	30	37.4	0.7

4.3 X-Ray Diffraction

XRD is the most widely used technique to determine crystal structure of a solid. In almost every study of ZrO_2 supported catalysts, the crystal structure of ZrO_2 was investigated in detail because it was closely related to the properties of catalysts.

XRD patterns for ZrO_2 are different Mo loadings calcined at 500 °C are shown in Figure 4.3. The X-ray diffraction spectra varied with molybdenum loading. Pure zirconia presented a typical monoclinic diffraction pattern, and with increasing Mo loading, the tetragonal phase was exhibited and became the dominant phase. Catalysts with over 1 at. % molybdenum demonstrated a similar signal, which suggests that ZrO_2 mainly exists in the tetragonal phase above this concentration level (Ramaroy et al., 2004).

In present study, the catalysts with Mo atomic loading from 0 % and 7 % were mainly investigated. In Figure 4.4, a closer examination of the XRD is presented for the samples with 0 and 7 at. % Mo and compared to a reference spectrum (Calafat et al., 2000). Pure zirconia showed very strong and dominant monoclinic characteristics, which is in agreement with previous reports (Calafat et al., 2000; Maity et al., 1999; Bhaskar et al., 2001). For catalysts containing 3 at. % Mo, the mixture of monoclinic and tetragonal was observed, but relative intensity of tetragonal peak was greatly increased compared to pure zirconia.

XRD was not able to detect molybdenum oxide when Mo loading was at low level because the size of MoO_3 crystallites (< 4nm) was smaller than detection limit (Bhaskar et al., 2001). When the Mo loading exceeded 7 wt. %, the diffraction line due to molybdenum oxide was found. In general, it can be drawn that Mo induced the transition of ZrO_2 from monoclinic to tetragonal over the range of compositions studied.

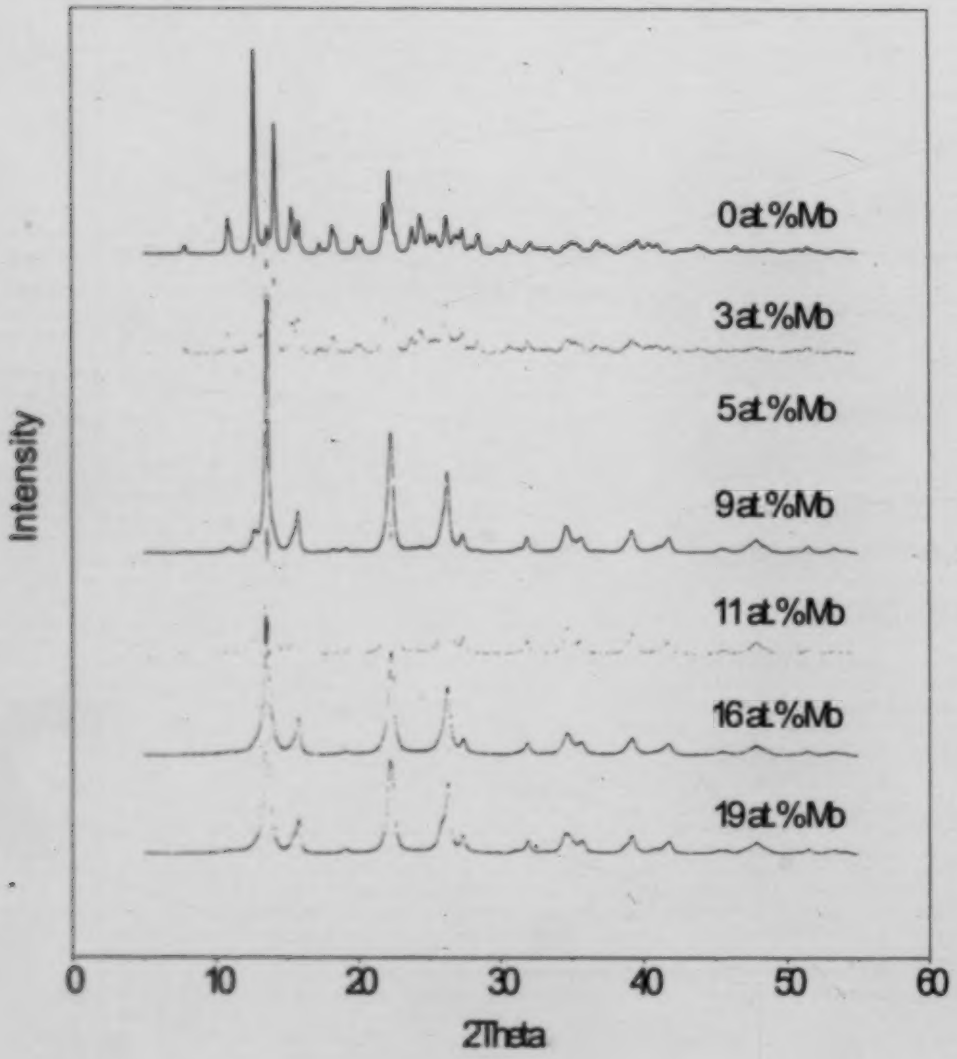

Fig. 4.3 High-resolution XRD Patten for ZrO_2 - MoO_3 without Ir Catalysts

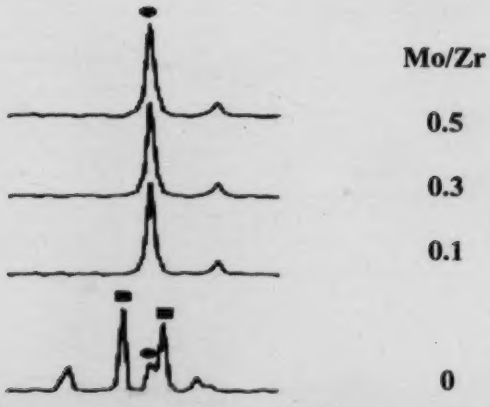

Fig.4.4.A XRD patterns of MoO_3/ZrO_2 catalysts obtained by co-precipitation and calcined at 500 °C (●) Tetragonal ZrO_2; (■) monoclinic ZrO_2.
(Reprinted from Calafat et al., 2000)

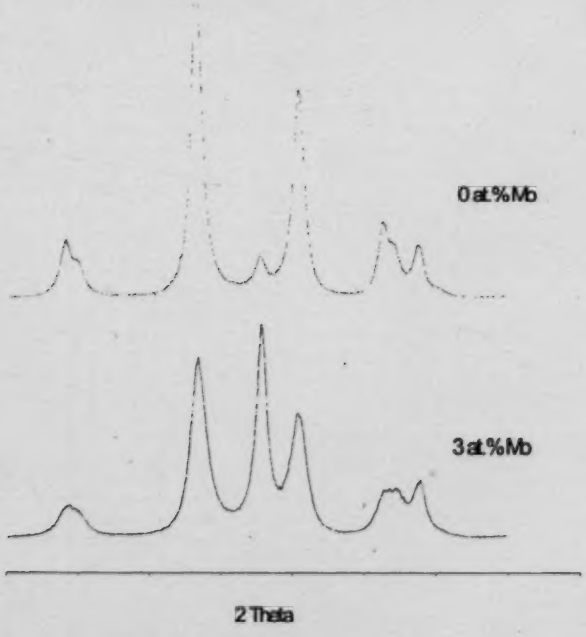

Fig. 4.4.B XRD pattern of catalysts with low Mo loading

4.4 Results of Temperature Programmed Techniques

4.4.1 Temperature Programmed Reduction (TPR)

In the present study, TPR analysis was performed from ambient temperature to the calcination temperature (500 °C). The reduction profile above this temperature was not studied in order to avoid possible crystal structure changes since the catalysts were calcined to this temperature.

The TPR profiles of Ir/ZrO_2-MoO_3 with 300 ppmw iridium are presented in Figure 4.5. The profiles suggest that the reduction mainly occurs in two regions. The first peak was observed at the region from 230 to 250 °C, and second peak was between 415 °C and 425°C. The increasing hydrogen uptake (area under peaks) suggests that the reducibility increases with an increase in the molybdenum loading. It was also noted that the introduction of Mo led to a slight shift of peak temperature, which was attributed to the interaction between ZrO_2 and MoO_3. These findings agreed with the results achieved by Ono et al. (1989). Kenny (2004) reported a two-peak spectrum for ZrO_2/MoO_3 catalysts with Mo greater than 5 at. % and one-peak spectrum for Mo below that loading.

A three-peak spectrum was observed when the Mo loading was 5 at. %. The third peak was observed at about 350 °C, and the area under the peak was increased for the catalyst containing 6.7 at. % Mo. The peak could be assigned to reduction of a new molybdenum compound. According to Calafat et al. (2000), they reported co-precipitation method favored the interaction of Mo and Zr, and the subsequent formation of a new Mo-Zr compound. No reduction peaks due to iridium oxides were observed in the present study, which is attributed to the low iridium concentration making it difficult to differentiate between its reducible peak and noise.

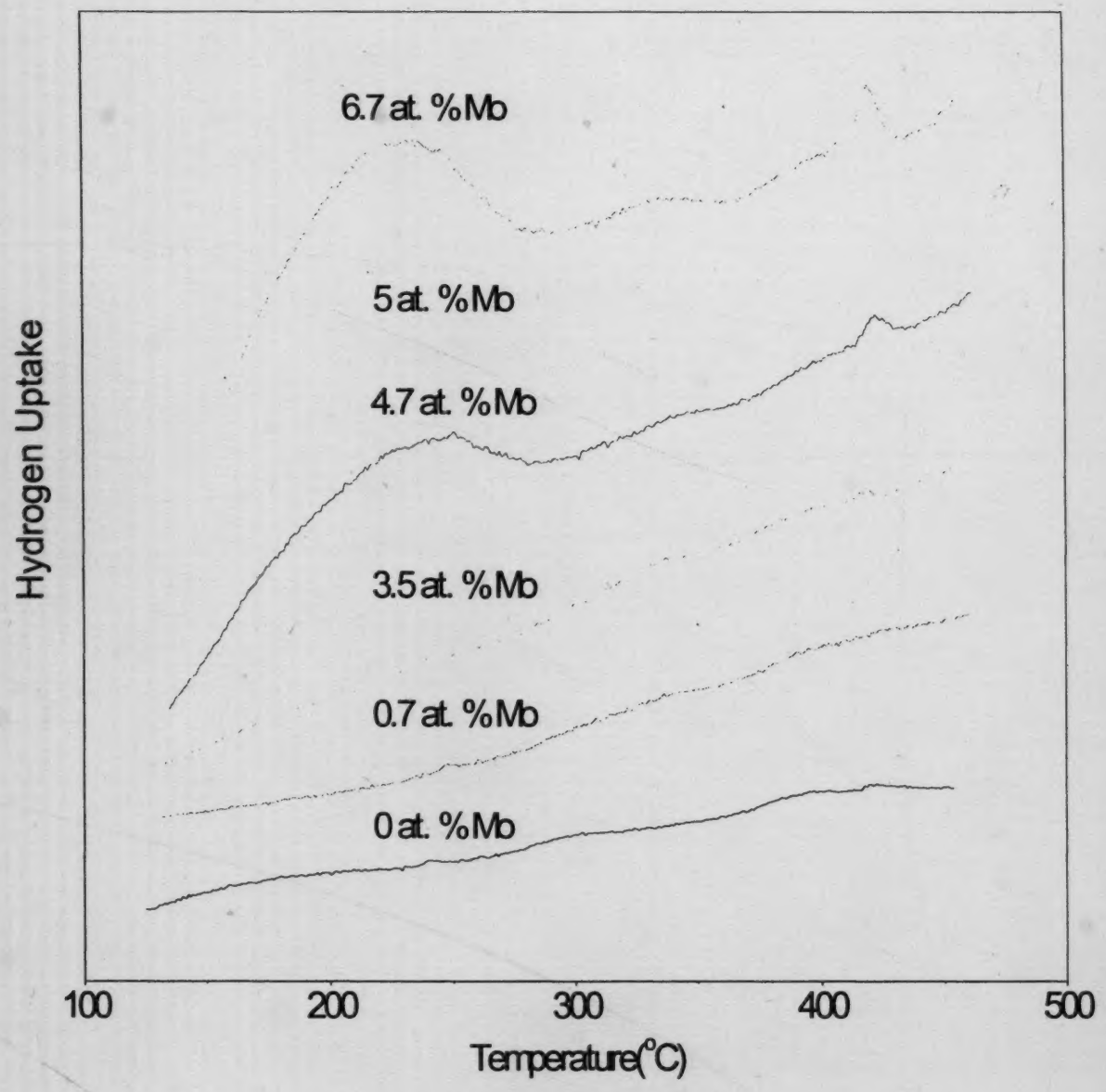

Fig.4.5 TPR profile of Ir/ZrO_2-MoO_3 catalysts

4.4.2 NH_3 Temperature Programmed Desorption (TPD)

Temperature programmed desorption (TPD) of ammonia was used to determine the number and strength of acidic sites. Ammonia was selected as probe molecule due to its small molecular size, stability and strong basic strength (pKa = 9.2) (Bhaskar et al., 2001). The ammonia TPD profiles of Ir/ZrO_2-MoO_3 catalysts at a desorption temperature rate of 45 °C/min are shown in Figure 4.6. It can be noted that the acidic sites were mainly in two regions. One region was a very broad range from 110 °C to 430 °C. It was believed that this broad peak was the sum of at least two peaks whose T_ms were around 220 °C for the weak acid sites and 370 °C for moderate acid sites. The T_m for strong acid sites was about 470 °C. The amount of ammonia desorbed corresponding to the acidic sites is given in Table 4.3. It was found that the number of acidic sites increased with molybdenum loading.

Figure 4.7 shows the TPD profile for a catalyst containing 0 at. % Mo at various temperature desorption rates from 25 °C/min to 45 °C/min. It can be observed that the maximum peak temperatures (T_m) shifted to higher temperatures with increasing ramp rates, as expected. The positions of the peak maximums were determined, and the heat of desorption (H_d) was calculated by applying the method described in Chapter 3. The same procedure was applied to all of the catalysts, and the obtained the heat of desorption values are listed in Table 4.4. From the calculated values, it is noted that the heat of desorption for three acid sites increased with increasing Mo loading, reaching the maximum values of 76.3, 135.8 and 172.2 J/mol for weak, moderate and strong acidic sites at 3.5 at. % Mo, respectively, and decreased beyond this composition. The change is

more significant at weak and moderate acid sites than the strong acid site, where the heat of desorption was similar among all catalysts.

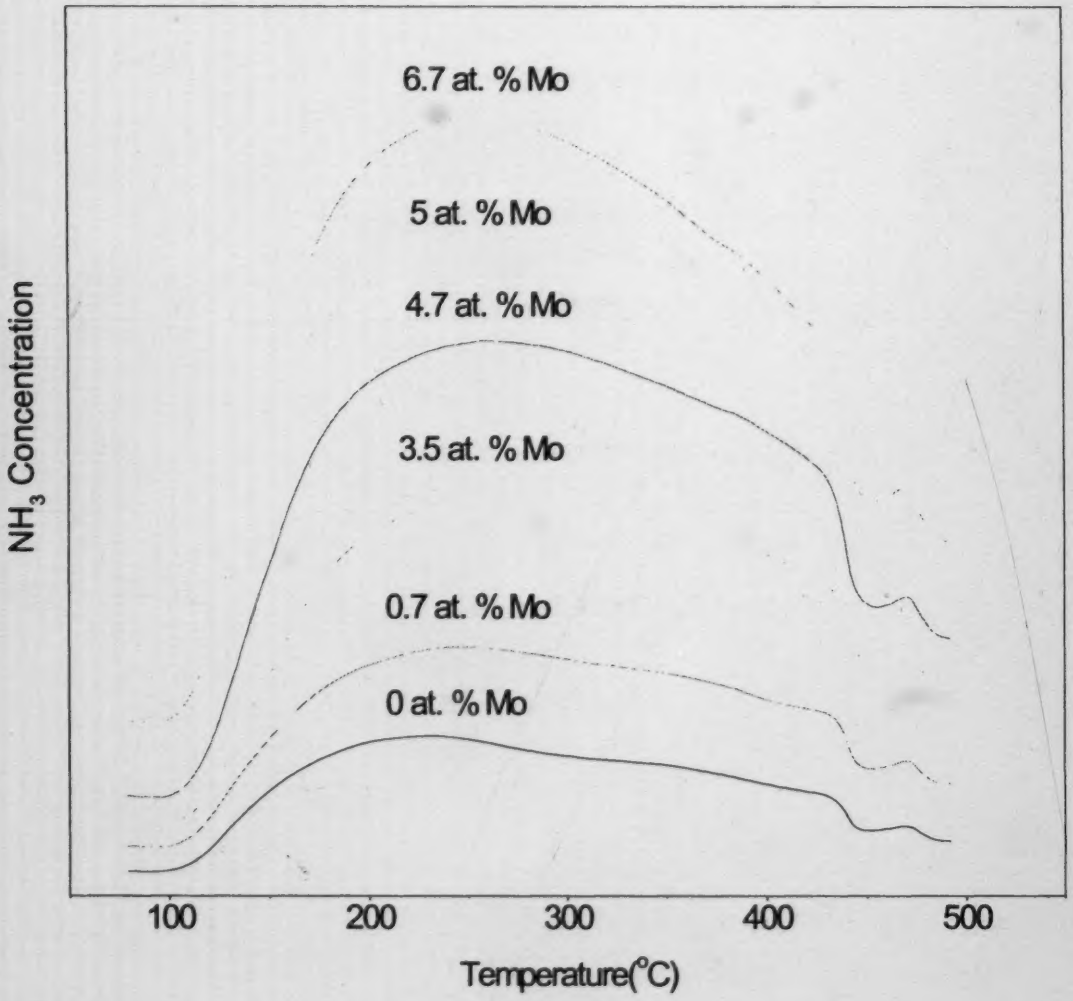

Fig. 4.6 NH_3 TPD profile of Ir/ZrO_2-MoO_3 catalysts at 45 °C/min

Table 4.3 Desorbed amount of ammonia for different acid sites on Ir/ZrO_2-MoO_3

Mo Atomic Loading	First T_{max} (°C)	Desorbed NH_3 (ml/g_{cat})	Second T_{max} (°C)	Desorbed NH_3 (ml/g_{cat})	Third T_{max} (°C)	Desorbed NH_3 (ml/g_{cat})
0 %	231	4.9	360	2.1	468	0.6
0.7 %	246	5.8	371	2.2	471	0.8
3.5 %	273	7.6	395	3.1	476	1.2
4.7 %	264	9.4	390	4.4	468	1.5
5 %	262	12.0	386	5.2	470	1.7
6.7 %	254	17.6	377	9.1	468	2.7

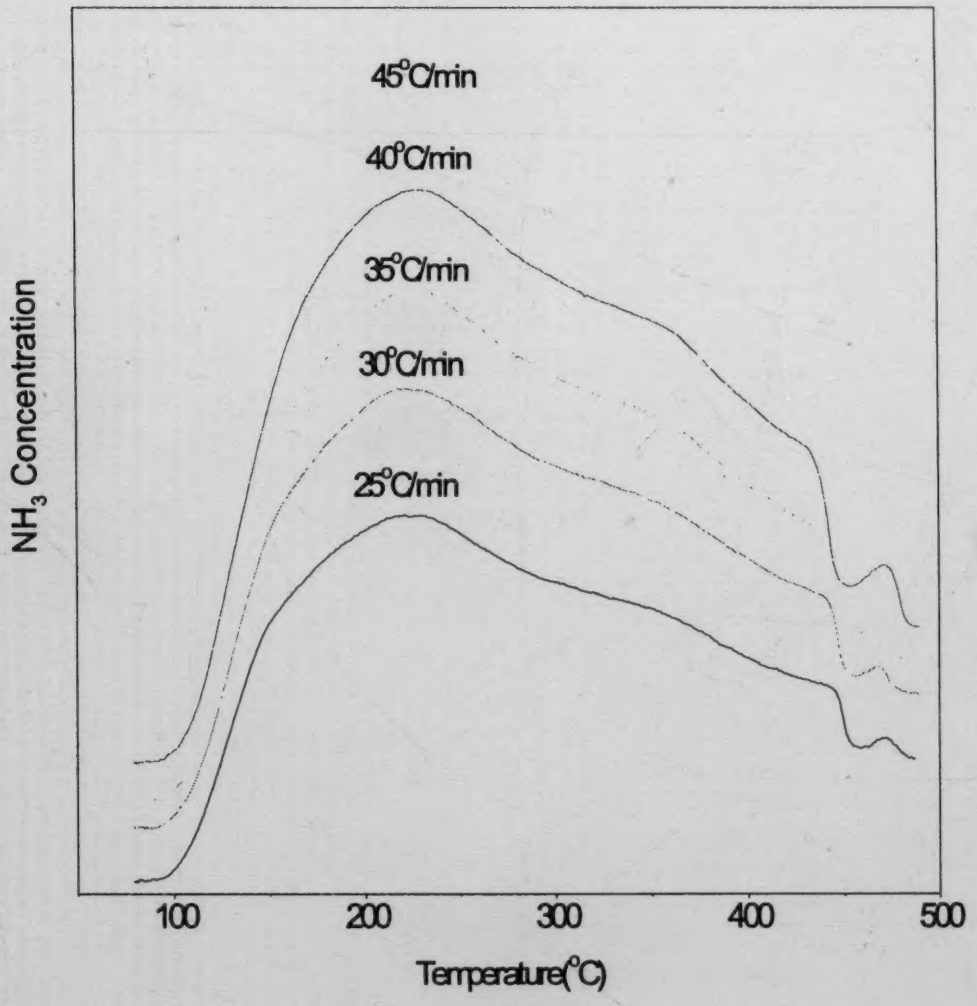

Fig. 4.7 NH_3 TPD profile of 0 at. % Mo at different heating rate

Table 4.4 Heat of desorption for different acid sites in Ir/ZrO_2-MoO_3 catalysts

Mo Atomic Loading	Heat of Desorption (J/mol)		
	Weak Site	Moderate Site	Strong Site
0 %	30.8	99.2	164.4
0.7 %	37.0	104. 2	167.1
3.5 %	76.3	135.8	172.2
4.7 %	58.3	124.3	163.3
5.0 %	54.1	118.6	165.6
6.7 %	42.9	109.2	162.1

4.4.3 CO Chemisorption

CO chemisorption was used to determine the iridium dispersion according to the amount of adsorbed CO and metal weight fraction. Figure 4.8 presents the profile of CO chemisorption for a catalyst containing 5 at. % Mo and 325 ppmw Ir. The area increased until the last two peaks had the same area. Because the area under peaks was proportional to the amount of unconsumed CO, it suggested that the CO was continuing to adsorb on the metal sites until saturation was reached, as evidenced by a constant peak area. Table 4.5 presents the estimated iridium dispersion and particle size for the catalysts prepares in the present study. It should be pointed out that the assumption that the stoichiometry of CO to metal site adsorption of 1:1 was made in the present study to determine iridium dispersion and particle size.

Table 4.5 Iridium dispersion for Ir/ZrO_2-MoO_3 catalysts (300 ppmw Ir)

Mo Atomic Loading	Iridium Dispersion (%)	Particle Size (nm)
0 %	33.3	3.3
0.7 %	30.3	3.6
3.5 %	6.1	18.0
4.7 %	10.6	10.4
5 %	48.0	2.3
6.7 %	12.9	8.5

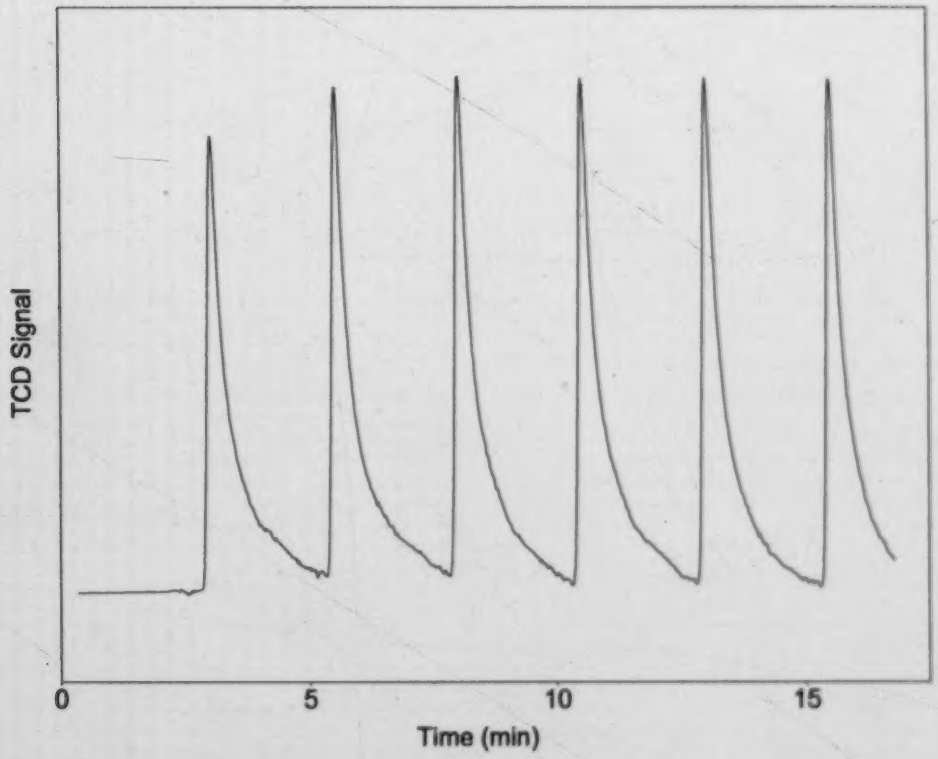

Fig. 4.8 CO chemisorption profile of 5 at. % Mo catalyst

4.4.4 BET Surface Area Measurement

BET surface area was measured by using the method described in Chapter 3. Two tests for each catalyst were performed and the average values were taken. The results are shown in Table 4.6. In general, the BET surface area increased with increasing Mo loading, which is in good agreement with previous studies.

Table 4.6 BET surface area results for catalysts with Ir at 300 ppmw level

Mo Loading (at. %)	BET Surface Area (±4%) (m^2/g)
0 %	15.3
0.7 %	18.6
3.5 %	20.9
4.7 %	21.6
5 %	25.3
6.7 %	26.2

4.5 Catalytic Activity and Selectivity

4.5.1 Methylcyclopentane Conversion

In current study, methylcyclopentane (MCP) conversion was performed at 350 °C and atmospheric pressure on Ir/ZrO$_2$-KMnO$_4$ with 300 ppmw S as an initial proof-of-concept study. The reaction was performed in a pulse mode, and the effluent stream was monitored by mass spectrometer. The intensity versus time for m/z = 41 was plotted, the area under the peaks was integrated, and average area was calculated. The reason for selecting m/z = 41 is that this peak was easily discernible in the mass spectrum. By observing the disappearance of MCP with and without the presence of a catalyst, the conversions for various catalysts were calculated. The results are presented in Table 4.1.

It can be observed from the results that very low MCP conversion was obtained for iridium-free catalysts. When iridium was introduced into the catalysts, the conversion greatly increased for all the catalysts. As 300 ppmw S was added, the conversion changed from 4 % to 95 % for catalyst with 1 at. % Ir, suggesting that MCP conversion correlates well with iridium loading, whereby the introduction of iridium improved the catalytic activity greatly. The trend may be attributed to the change of reaction mechanism from Hugg-Dixons mechanism to classical bifunctional mechanism (Garcia et al., 2002).

For pure zirconia, the conversion did not increase significantly before and after iridium was added, remaining essentially zero in both cases. Therefore, the conversion is not only related to metallic sites, but also other factors, such as acidity. According to TPD results, both the number and strength of acidic sites for pure zirconia catalyst were the lowest for all catalysts. With increasing molybdenum, the conversion increased to 70.2 %

at 3.5 at. % Mo, where the strength of acidity reached the maximum and the Ir concentration was much higher than that at 0.7 % Mo resulting in a significant increase in MCP conversion. However, the catalyst with 4.7 at. % Mo gave a very low conversion (13.8 %), and beyond the point, MCP conversion reached the maximum value (95.2 %) at 5 at. % Mo. In this initial proof-of-concept study, selectivity was not studied.

Table 4.7 Comparison of conversion results for catalysts with and without Ir

Mo Loading (at. %)	MCP Conversion (%)		Ir concentration (ppmw)
	Without Ir	With Ir	
0 %	0.1	1.3	349
0.7 %	2.6	18.0	247
3.5 %	1.2	75.4	409
4.7 %	6.7	13.8	340
5.0 %	4.0	95.2	325
6.7 %	0.6	80.3	336

4.5.2 Cyclohexane Conversion

The ring opening reaction of cyclohexane (CH) was performed on Ir/ZrO_2-MoO_3 catalysts under 7 MPa H_2 pressure and 400 °C. The distribution and relative intensity of products were determined by GC-MS, as shown in Figure 4.9. It was noticed that n-alkanes with different carbon numbers were the dominant products in the current study. It was noted that both cyclohexane and hexadecane (solvent) contributed similar reaction products. Therefore, a series of control experiments with hexadecane-only were performed to determine the relative contribution to the product spectrum arising from hexadecane cracking, and the reported values are corrected for this observed phenomenon.

Figure 4.10 and Figure 4.11 give the relationship between the selectivity to n-hexane and activity and catalyst composition, respectively. The selectivity was defined as weight ratio of n-hexane to total products. It was assumed that hexadecane and cyclohexane did not interact each other, and there was no secondary hydrocracking.

From Figure 4.10, it can be noted the selectivity reached the maximum value (37.6 %) using the control catalyst of Ir/Al_2O_3 with 332 ppmw Ir. However, the maximum selectivity occurred at 3.5 at. % Mo for 30 ppmw level catalysts. This clearly illustrates the importance of balancing the metallic and acidic functionalities for maximizing activity and selectivity. For catalysts with 300 ppmw Ir, the selectivity reached the maximum value (30.3 %) at the catalyst with 4.7 at. % Mo, and then decreased with increasing Mo loading to 13.4 % at 6.7 at. % Mo. The selectivity was close to zero for pure zirconia. On the other hand, 30 ppmw catalysts presented a different trend. The

maximum selectivity to n-hexane of 21.3 % was observed for the catalyst with 3.5 at. % Mo, followed by a decreasing trend with increasing Mo loading.

Figure 4.11 illustrates the correlation of the activity with composition. It should be noted that the conversion was defined as CH disappearance. Similar to selectivity, the activity increased with Mo loading. Pure zirconia gave a conversions of 27.6 % and 2.4 % at 32.3 ppmw and 349 ppmw Ir, while the catalysts containing 5 at. % Mo had conversions of 32.6 % and 16.2 % with 31.5 ppmw and 325 ppmw Ir, respectively. Beyond this Mo loading, the conversion decreased with increasing Mo loading to 28.7 % and 14.6 % at 6.7 at. % Mo with 41.8 ppmw and 336 ppmw Ir. The conversion using pure zirconia was slightly higher than that of 0.7 at. % Mo for 30 ppmw Ir loading. It is interesting to note that the conversion for 300 ppmw catalysts was lower than that for 30 ppmw catalysts, which implies that increasing metal concentration depressed the activity. In general, the activity and selectivity could be attributed to the balanced effect of two functionalities in catalysts, acidity and metallic functionality.

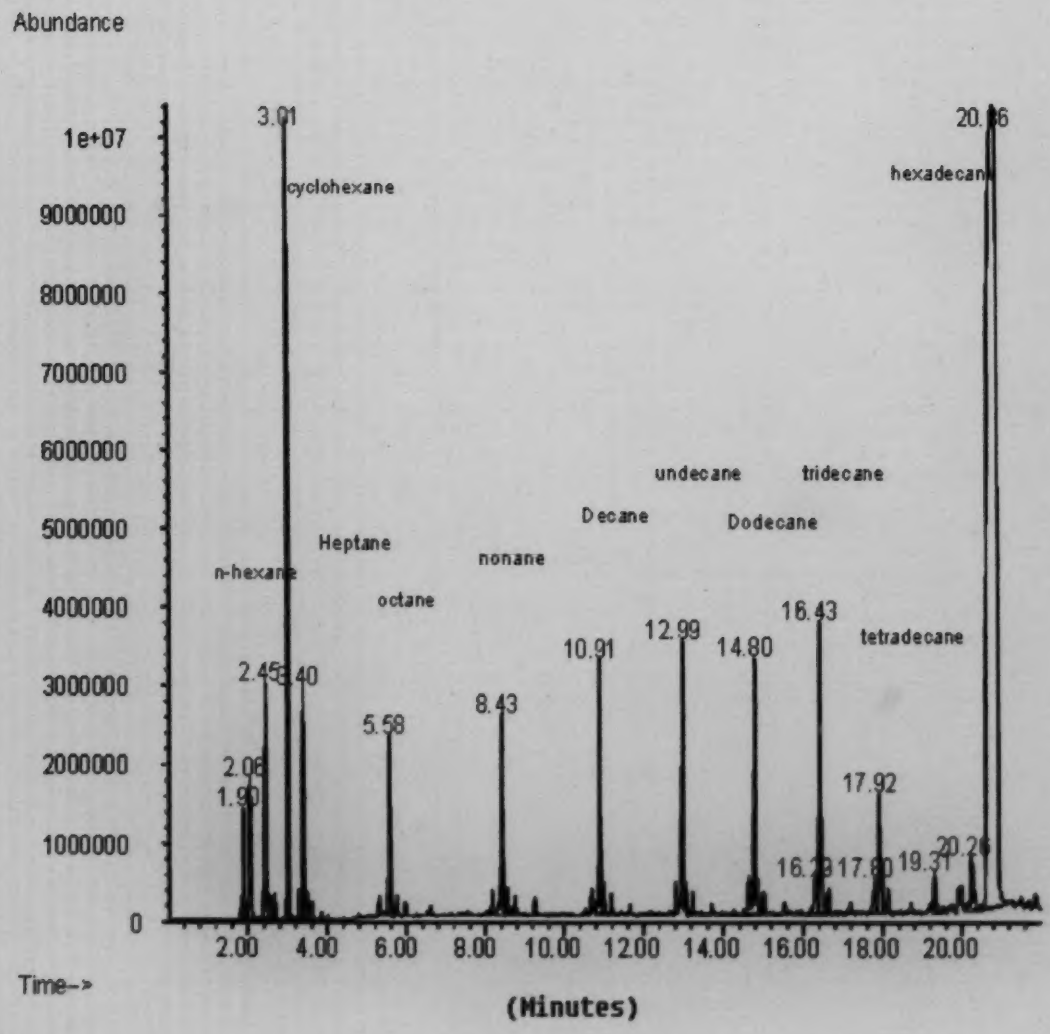

Fig.4.9 Products GC Spectrum for catalyst with 0.7 at. % Mo and 38 ppmw Ir

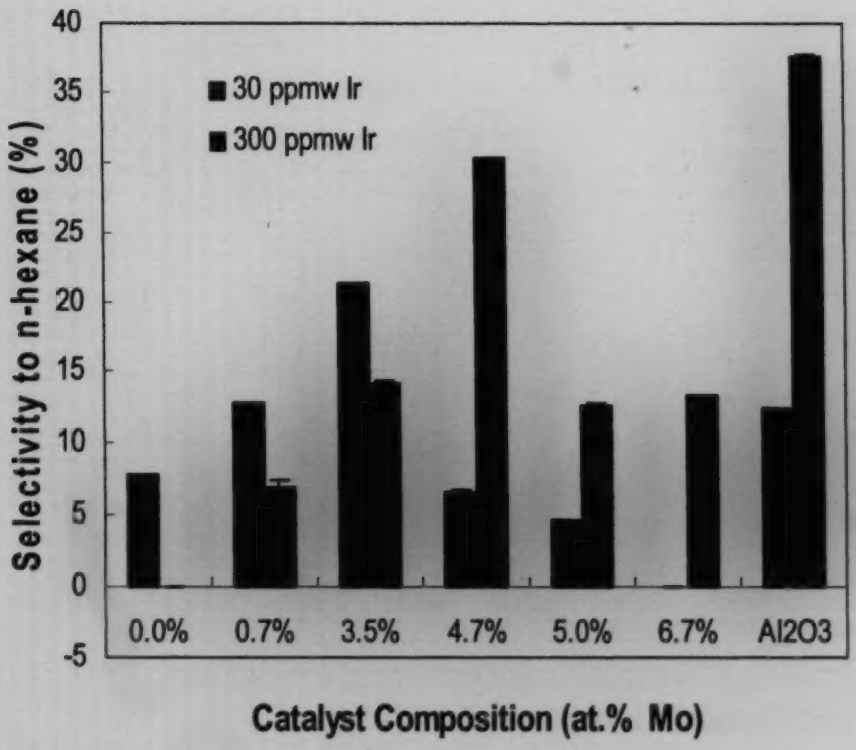

Fig.4.10 Selectivity to n-hexane as function of catalyst composition (400 °C, 7 MPa H_2)

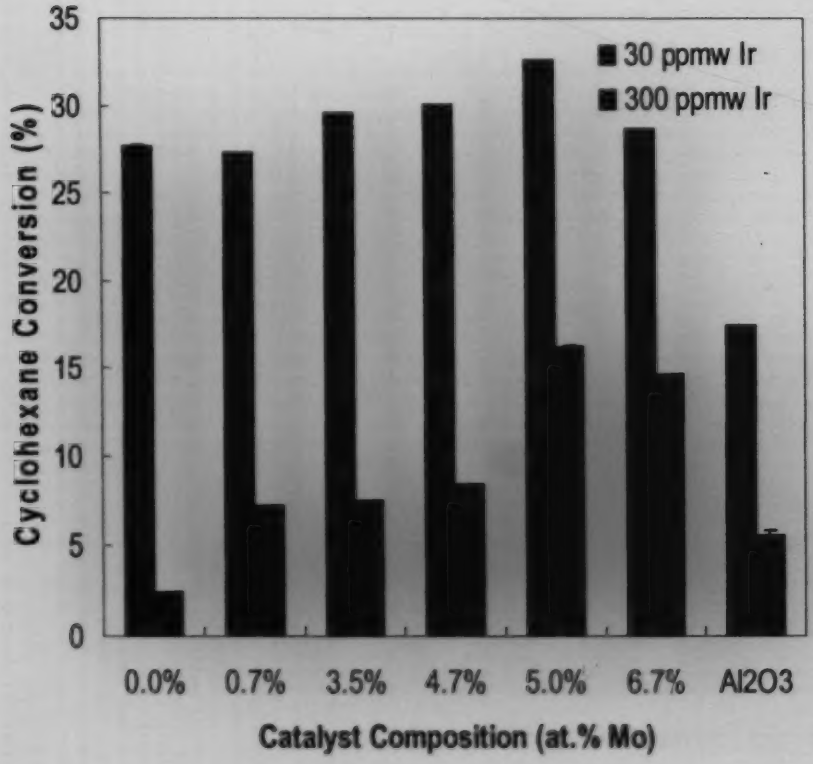

Fig.4.11 Activity as function of catalyst composition (400 °C, 7 MPa H_2)

CHAPTER 5

DISCUSSION

5.1 X-Ray Photoelectron Spectroscopy (XPS)

In this study, XPS was used to determine the Mo loading and oxidation state of the metals. From the survey scan spectra, all examined elements except iridium were identified, which was due to the extremely low iridium concentration (30 and 300 ppmw). Therefore, INAA (Instrument Neutron Activation Analysis) was used in this study.

From Table 4.1, a binding energy shift for all elements was observed, which could result from the elemental oxidation state, chemical bonds, crystal structure, or a charged sample. If a sample was charged, the electron intensity around atoms changed correspondingly. For example, the electron intensity of oxygen increased when a sample was charged. Therefore, the kinetic energy of emitted electron became higher due to higher repulsive force. According to energy balance, the binding energy decreased and shifted to lower value, which was seen from Table 4.1.

The difference between the adjusted binding energy and reference binding energy was calculated. It was noted that the direction and magnitude of the binding energy shift for Mo and Zr varied for each catalysts, which implies the interaction of Mo and Zr slightly changed with increasing Mo loading. Although the shift varied with Mo loading, the binding energy of $3d_{5/2}$ in catalysts was higher than that in the pure metal (Mo $3d_{5/2}$ = 228 eV; Zr $3d_{5/2}$ = 179 eV) due to the chemical shift.

5.2 X-Ray Diffraction

There are three main crystal structures for ZrO_2; monoclinic, tetragonal and cubic. Maity et al. (2000) examined the XRD patterns for pure ZrO_2 and ZrO_2-MoO_3 with up to 10 wt. % Mo, and found that the zirconia monoclinic phase transformed to a tetragonal phase with the addition of molybdenum, which agrees with the observation in current study. They also noted that a molybdenum oxide pattern was observed above 6 wt. % Mo loading and the area under the peak increased with Mo loading. The similar observation was found in another study (Afanasiev et al., 1995).

From Figure 4.4, an increasing relative intensity of the tetragonal peak with increasing Mo content was observed. The results reported by Catafat et al. (2000) indicated that Mo opposed the transition of ZrO_2 from the tetragonal to monoclinic phase, and they argued that the tetragonal phase was stable when the zirconia grains were lower than a critical size. However, they also pointed out another change for samples calcined at 700 °C; the Mo was effectively preventing this structural transition, and the transition was expected to occur with increasing Mo loading. Furthermore, Catafat et al. (2000) studied catalysts with higher Mo loading (up to 50 at. %). $Zr(MoO_4)_2$ was formed at high MoO_3 content for catalysts prepared by co-precipitation method and calcined at 700°C.

The phase formation of ZrO_2 in ZrO_2-MoO_3 is not only related to the Mo loading, but also other factors, such as calcination temperature, and preparation procedure. Catafat et al. (2000) pointed out that ZrO_2-MoO_3 showed a mixture of tetragonal and monoclinic with a 0.1 Mo/Zr ratio when the catalysts were prepared by co-precipitation and calcined at 700 °C. Furthermore, the increase in the Mo/Zr ratio made the microstructure of ZrO_2 become monoclinic, which was not observed in the catalysts calcined at 500 °C. If the

procedure of late Mo addition was adopted to make catalysts, ZrO_2 was mainly in the tetragonal phase, regardless of what calcination temperature was used. Xie et al. (2000) reported that ZrO_2 transformed from tetragonal to monoclinic when the samples were exposed to moist ambient air at room temperature.

5.3 Temperature Programmed Techniques

5.3.1 Temperature Programmed Reduction (TPR)

According to the TPR pattern in Figure 4.5, the tendency of hydrogen uptake with molybdenum loading was not only due to the increasing Mo loading, but also the phase change of molybdenum oxide. Maity et al. (2000) pointed out that molybdenum oxide mainly existed as a tetrahedral species at low Mo loading, which was difficult to reduce because of the strong interaction with ZrO_2. With increasing Mo loading, tetrahedral and octahedral phases were reduced more easily. Therefore, the two reduction peaks could be assigned different phases of Mo oxides. The peak at low temperature could be the reduction of the octahedral species, while the peak at high temperature is attributed to the reduction of tetrahedral species.

Pure zirconia was not reducible over the temperature range studied. Maity et al. (2000) noted that pure zirconia was not reduced except at very high temperatures of about 726 °C. With the addition of Mo, no reduced peak for ZrO_2 was observed, which implies that Mo suppressed the reducibility of ZrO_2. Bhaskar et al. (2001) also studied the reduction of zirconia to higher temperatures of 1000 °C, but no reduction peak was observed. No reducible peak was observed in current study. This further suggests that the observed reduction peaks are due to the reduction of molybdenum oxide species.

With increasing Mo loading to 5 at. %, a three-peak spectrum was observed. The three peaks are assigned to the reduction of bulk MoO_3 (230 °C), MoO_2 (420 °C), and a new molybdenum oxide (340 °C) formed due to increasing Mo content respectively. Other factors that could affect the TPR patterns include calcination temperature and the method of preparation (Calafat et al., 2000).

5.3.2 NH_3 Temperature Programmed Desorption (TPD)

Temperature programmed desorption (TPD) of ammonia is widely used to determine the number and strength of acid sites. In Figure 4.6, the ammonia TPD profiles of Ir/ZrO_2-MoO_3 catalysts at 45 °C/min showed three acidic sites with different strength mainly in two regions. Kenney (2004) studied the acidity of ZrO_2-MoO_3 catalysts without iridium, and reported similar TPD patterns. However, the peak temperatures were lower than those observed in this study, which could be attributed to the introduction of Ir, which may have enhanced the interaction between MoO_3 and ZrO_2 and caused higher reducible temperatures.

The results in Table 4.3 indicate the amount of acidic sites increased with molybdenum loading from 7.6 ml/g_{cat} at 0 at. % Mo to 29.4 ml/g_{cat} at 6.7 at. % Mo. Bhaskar et al. (2001) reported that the acidic sites existed in two regions in 300 °C and 550 °C, and the acidity increased with increasing Mo loading. In addition, Kenny (2004) calculated the desorbed ammonia per unit catalyst mass and unit surface area, and found that the transition from monoclinic to tetragonal structure greatly affected the acidity. The desorbed NH_3 volume decreased for monoclinic phase, and was almost constant in the tetragonal phase.

The heat of desorption (H_d) was calculated based on TPD data under different ramp rates, and is summarized in Table 4.4. The H_d reached the maximum values of 76.3, 135.8 and 172.2 J/mol for weak, moderate and strong acidic sites at 3.5 at. % Mo, and decreased beyond the point. It should be noted that each peak identified in the study includes many acidic sites with similar but different heats of desorption, which are related to the local structure of surface the acidic sites are bonding with. Therefore, the calculated heats of desorption was an average value for the supported catalysts (Blyholder et al., 1964).

5.3.3 CO Chemisorption

Several early experiments investigated CO adsorption on iridium (Hoffmann, 1988). The photoelectron spectra of three different systems, free CO, an iridium carbonyl – $Ir_4(CO)_{12}$ – cluster, and CO adsorbed on an Ir (1 0 0) surface, were compared (Zaera, 2001). According to Figure 5.1, the peaks corresponding to the 4σ and 1π can be seen, while the peak for 5σ orbital was not detected in the last two systems compared the free CO, which indicated the bonding orbital was 5σ. The Blyholder model in surface science was well developed to explain it (Blyholder, 1964).

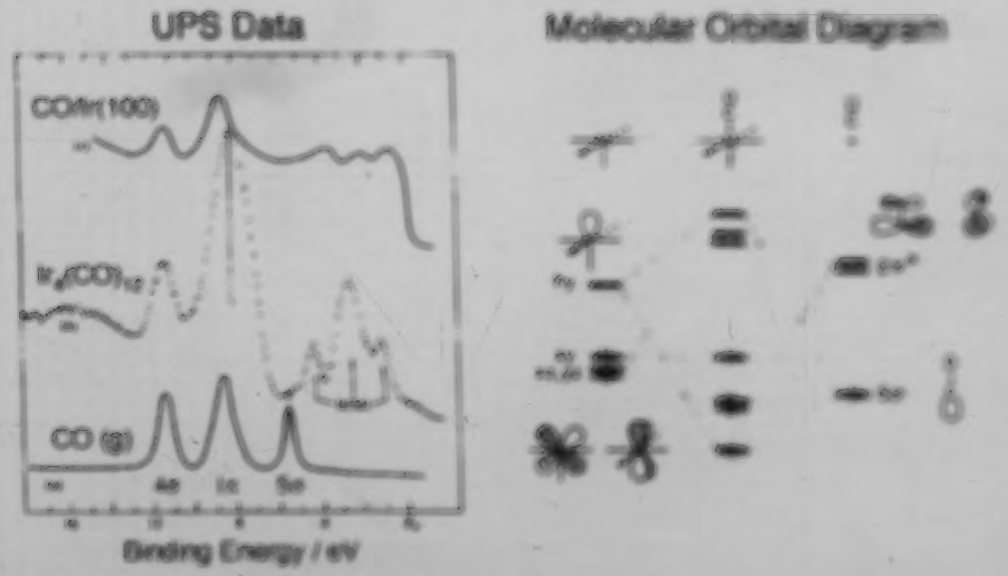

Fig. 5.1 UPS patterns for CO in the gas phase, bonded to an iridium cluster, and absorbed on an iridium surface
(Reprinted from Zaera, 2001)

Iridium is present as a metal oxide present both on the surface and in the bulk structure because it was calcined in air at 300 °C after impregnation. The iridium dispersion for all samples is listed in Table 4.1. It can be observed that the metal dispersion varied with each sample, which was mainly contributed to the preparation of Ir impregnation. The iridium particle size increased with Mo loading, and reached 10.0 nm at 3.5 at. % Mo and decreased to 2.3 nm at 5 at. % Mo. However, a particle size of 0.3 nm occurred at 6.7 at. % Mo. Therefore, a clear correlation between the metal particle size and Mo loading was not observed. According to the results of CH conversion in this study, the conversion for 300 ppmw catalysts was lower than that for 30 ppmw catalysts. It could be attributed to that more iridium reduced the amount of accessible acidic sites by forming larger metal cluster sizes.

5.3.4 BET Surface Area Measurement

An increase of BET surface area (Table 4.1) with Nb loading was observed, which agrees with the results of Kuwabara (2004) and Ghodbhe et al. (2009). Zhao et al. (1997) also reported that the surface area of ZrO$_2$ by adding Nb$_2$O$_5$ was larger than that of pure ZrO$_2$. The change can be explained by the fact that the introduction of Nb enhance the crowning and grain growth rate of ZrO$_2$ by forming a two-dimensional layer on the surface of the zirconia particles (Ghodbhe et al., 2009). This explanation is also supported by the work performed by Gopalan et al. (1991). Sintering and grain growth were the main mechanisms that affect the surface area of ZrO$_2$ in the temperature range from 40 to 600 °C (Gopalan et al., 1991). From the view of crystal structure, the presence of Nb opposed the transition from tetragonal to monoclinic and led to the high surface area (Ghodbhe et al., 2009).

A maximum surface area was reached and then the surface area began to decrease with increasing Nb loading. The decrease beyond a certain Nb/Zr molar ratio of 0.1 for co-precipitation method was caused by the formation of a pure Nb$_2$O$_5$ phase, or possibly stronger interactions between Nb and O at high Nb loading. The formation of crystalline Nb$_2$O$_5$ was favored and blocked the pores of zirconia (Ghodbhe et al., 2009). However, the Nb$_2$O$_5$ ratio at which the maximum surface area occurred varied with the employed preparation method (Ghodbhe et al., 2009).

5.4 Catalytic Activity and Selectivity

5.4.1 Reaction Pathways

In the study of cycloalkane ring opening reaction, two basic mechanisms are generally recognized, i.e. a classical bifunctional mechanism and a Haag–Dessau cracking mechanism (Raichle et al., 2001). The alkylcyclohexane in the present study was selected to illustrate the two different schemes, where the carbon number of substituent was usually less than 5.

In a typical bifunctional pathway, which is shown in Figure 5.2, the alkylcyclohexane is dehydrogenated on metallic sites to form alkylcyclohexene. The alkylcyclohexene is protonated on acidic sites. Ring contraction, i.e. isomerization, greatly affects ring-opening rates and selectivity. Therefore, controlling the conversion between six-membered rings and five-membered rings becomes very important to develop a bifunctional catalyst. After ring contraction, the β-scission proceeds to produce branched olefins. The resulting olefins are hydrogenated on metallic sites to form branched alkanes.

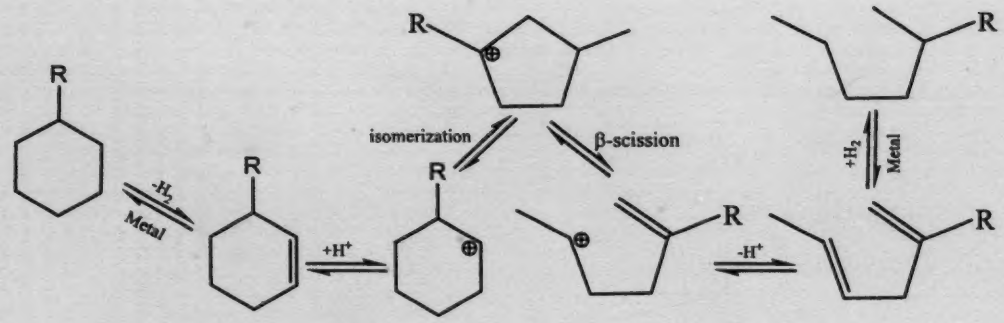

Fig.5.2 Classical bi-functional mechanism for selective ring opening

(Adapted from Raichle et al., 2001)

For the Hagg-Dessau mechanism, the alkylcyclohexane is directly protonated on acidic sites without undergoing dehydrogenation. The formed carbonium ion possesses a structure with a three-center, two-electron bond in the transition state (Raichle et al., 2001). Then the electron bond is cleaved to form an alkene, which is hydrogenated to produce an alkane on the metallic sites. This pathway is illustrated in Figure 5.3. This non-classical cracking route usually occurs to a low extent over a typical bifunctional catalyst, because this mechanism has a higher activation energy barrier (Raichle et al., 2001).

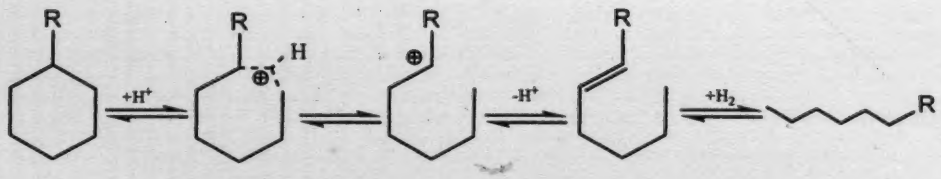

Fig.5.3 Haag-Dessau mechanism for selective ring opening

(Adapted from Raichle et al., 2001)

However, when the substituent on the ring was more than five carbon atoms, the yield of desired ring opening products is low, because the cracking of the endocyclic C-C bond is two to three orders of magnitude slower than that of exocyclic bond (Corma et al., 2001), which leads to excessive naphthene side-chain cracking.

5.4.2 Pulse Mode (MCP)

Methylcyclopentane (MCP) is a common probe molecule to study the mechanism and energetics of selective ring opening. For Pt catalysts, the selectivity is very sensitive to particle size (Du et al., 2005). When Pt particle size is small, the MCP reaction underwent a non-selective mechanism and the ROP ratio followed statistical rule. With an increasing Pt loading, the selective mechanism was doiminant. Furthermore, the competing mechanism, a partially selective mechanism, co-existed at 10 % Pt/Al_2O_3 and high temperature. On the other hand, the ring opening of MCP on Ir was less sensitive to the particle size of metals compared to Pt containing catalysts (Galperin et al., 2003).

In this study, the reaction of MCP was used only as a proof-of-concept. From the results in Table 4.7, a significant increase in MCP conversion was observed due to the introduction of iridium. For the monofunctional catalysts (acidity), the reaction occurred only over acidic sites, and the MCP was not converted into an olefin and more likely followed a Hagg-Dessau mechanism, as illustrated in Figure 5.4. The lack of metallic function provided insufficient spillover hydrogen (Roessner et al., 1996) to the acidic sites to saturate the transitional carbenium ions. On the other hand, when Ir was incorporated, the bifunctional mechanism was dominant. The metal function enhanced hydrogen spillover to acidic sites to form saturated products, which further increased the conversion compared to metal-free catalysts.

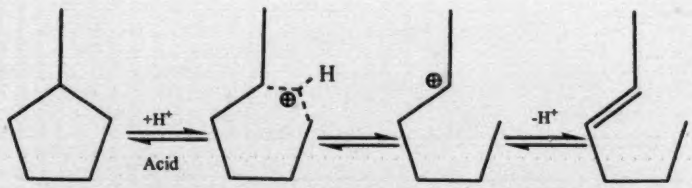

Fig.5.4 Ring opening reaction for MCP on ZrO_2/MoO_3

(Adapted from Raichle et al., 2001)

The activity and selectivity of MCP ring opening depends not only on the type of metal, particle size and crystal structure, but also the support acidity. For example, Galperin and co-workers (2003) studied how the support properties affected the ring opening reaction of MCP. If the support was acidic, the reaction was mainly the isomerization of MCP to cyclohexane followed by formation of aromatics, while the methylpentane and hexane were produced if the support was basic.

In the present study, it was observed that MCP conversion increased from close zero to 75.5 % when the Mo loading was changed from 0 at. % to 3.5 at.%, which was attributed to the amount and strength of acidic sites function in the examined compositional range. In addition, the Ir concentration for the catalyst containing 3.5 at. % Mo (409 ppmw) was much higher than that at 0.7 at. % Mo (247 ppmw), which led to a significant improvement of conversion. However, the catalyst containing 4.7 at. % Mo gave an abnormally low conversion (13.8 %), and beyond the point, the conversion reached the maximum value (95.2 %) due to continuous increase in the amount of acidic sites.

It should be emphasized that the ring opening reaction is a very complicated mechanism, and the activity of catalyst can be influenced by many factors. It is difficult to determine the dominant factor and elucidate the role of each factor to overall behavior of catalysts.

5.4.3 Batch Mode (MCH)

Ir supported catalysts were very effective to open five-membered rings, but six-membered ring opening is slower on these catalysts. McVicker et al. (2002) reported that the selectivity to the ring opening products of alkylcylohexanes was much lower than that of alkylcyclopentanes on noble metals such as Ir under the same conditions. They also observed that the SRO was much slower for six-membered rings than five-membered rings for all examined metals, Ru, Ni, Pt and Ir. Platinum only gave about 4 % selectivity to C_6-alkanes for MCH compared to 98 % for MCP. A compound with a six-membered ring requires ring contraction and β-scission in order for the ring opening reaction to

proceed, and DFT modeling work by Abraham (2005) proved that this was the rate determining step.

The ring-opening pathway for cyclohexane can be determined by analyzing the product distribution. For example, Weitkamp et al. (2001) suggested two ring-opening mechanisms for methylcyclohexane (MCH) on H-ZSM-5 zeolites catalysts. In a classical bifunctional mechanism, the MCH was dehydrogenated on metallic sites, and the cycloalkene was protonated to produce carbenium ions on acidic sites. The isomerization happened to form branched isomers, and then β-scission proceeded. The resulting diene was hydrogenated on metallic sites. In the other pathway called the Hagg-Dessau mechanism, the MCH formed a carbonium ion directly through protonation effect without dehydrogenation step. The bond formed with three centers was broken, and the ring was cleaved. In this case, n-alkanes were major products, which is in agreement with the GC spectra obtained in this study. Therefore, it seems that the Haag–Dessau mechanism is better to describe the selective ring opening reaction of cyclohexane over Ir/ZrO_2-MoO_3 catalysts than the bifunctional mechanism. However, thermodynamic aspects are another factor that need to be considered when deciding the more favorable pathway. According to Abraham (2005), the bifunctional mechanism was more energetically favorable than the Haag-Dessau mechanism for methylcyclohexane ring opening. Furthermore, the transitional carbonium ion with a three-center and two-electron bond in the non-classical mechanism was not observed in his study. Generally, the selective ring opening of cyclohexane can be described by the pathway in Figure 5.5.

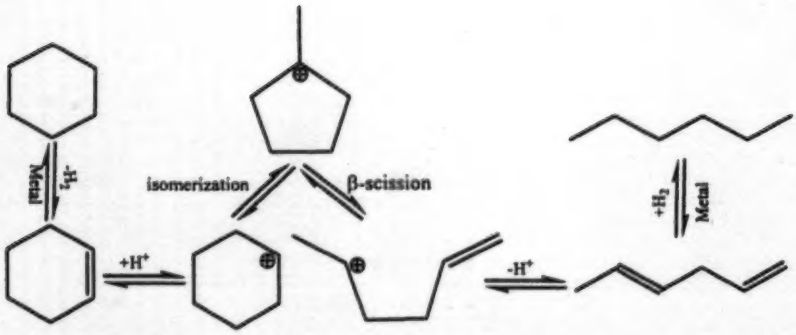

Fig.5.5 Classical bi-functional mechanism for CH on Ir/ZrO_2-MoO_3

(Adapted from Raichle et al., 2001)

The selectivity for n-hexane (Figure 4.10) demonstrated a similar pattern for both iridium loadings (30 and 300 ppmw), but compositions for the highest selectivity and the overall selectivity were different. This observation can be attributed the combining effect of metallic and acidic sites. According to the TPD results, the amount of acidic sites increased with Mo loading, and the maximum heat of desorption was obtained at catalyst containing 3.5 at. % Mo. In the range from pure zirconia to catalysts with highest selectivity, increasing acidic sites favored the selectivity to n-hexane by the improvement of protonation and ring contraction steps. Beyond that point, the acidic sites continued to increase, which resulted in the improvement of hydrocracking activity and lowered the yield of target products. According to the bifunctional mechanism, the acidic sites are not active for ring opening by themselves but greatly increase the ring contraction rate, and metal sites also play a very important role to increase selectivity by initiating the reaction and enabling dehydrogenation/hydrogenation ability. This synergy implies higher ring opening and hydrogenation ability and increases the ratio of the target product.

When two parts of Pt/USY by weight were added into one part of Ir/Al_2O_3, the yield of ring opening for methycylcohexane (MCH) was doubled and the cracking yield halved compared to an iridium-only catalyst (McVicker et al., 2002). It is observed from Figure 4.10 that high Ir concentration does not always give high selectivity for Mo content from 0 to 3.5 at. %. It can be explained that the acidic sites played a dominant role for ring opening in the compositional range in the present study. The selectivity for 30 ppmw Ir catalysts was lower than that for 300 ppmw Ir catalysts for Mo loading from 4.7 to 6.7 at. %, and this is suggested to be due to insufficient metal sites for dehydrogenation and hydrogenation.

An overall trend about activity (Figure 4.11) is the 30 ppmw Ir catalysts gave higher conversion than 300 ppmw Ir catalysts based on the same support materials, suggesting that high iridium loading suppressed the activity. McVicker et al. (2002) brought out the concept of effective acid sites, which was directly related to total conversion. Thus, besides the balancing effect of metal and acid functions, the incorporation of more iridium blocked some accessible acidic sites and reduced the conversion to some extent by forming larger metal cluster sizes. It should be pointed out that the total conversion includes cracking, ring opening and isomerization. Cracking almost certainly occurred under the current reaction parameters (400 °C and 8 hours). In addition, high conversion tended to occur at high Mo loading (5 at. %), where there were more acidic sites that contributed total conversion.

Based on the discussions above, it has been noted that the balancing metal and acid function plays a crucial role to determine the activity and selectivity of the catalysts. Acid function favors the activity and selectivity by improving the ring contraction rate.

However, too high acidity also leads to excessive cracking reactions, thereby the reduction of selectivity. Furthermore, the protonation step requires a proton, which is formed on Bronsted acid site by donating an electron from hydrogen. Spillover hydrogen is produced due to hydrogen dissociation on metal function. McVicker et al. (2002) systematically investigated the role of balanced acidity and metallic functionality for MCH ring opening. They found ring opening rate did not follow the same direction with selectivity when acidity in an ECR-32 based catalyst varied. Pentylcyclopentane (PCP) and n-butylcyclohexane (BCH) were also selected in their study. Iridium supported on USY and Al_2O_3 catalysts gave much higher selectivity and ring opening yield than platinum based catalysts for PCP reaction. For BCH, the addition of one part Pt/USY increased ring opening yield from 14 to 30 % for Ir/Al_2O_3. However, the yield decreased to 10 % when 3 parts of Pt/USY was added, though the total conversion was improved from 38 % to 70 %, which demonstrated the importance of the balance of metallic sites and acidic sites.

In general, the balance of acid and metal sites is very complicated and important to affect the performance of catalysts. The Al_2O_3 based catalyst gave the highest selectivity among 300 ppmw Ir catalysts, while this was not the case for 30 ppmw Ir catalysts. An optimum balancing effect needs to be determined by experiments and clarifying the interaction of the two functions.

CHAPTER 6

CONCLUSIONS

6.1 Conclusion

The objective of this study was to prepare catalysts combining the hydrogenation and hydrogenolysis activity to promote selective ring opening. The key issues associated with Ir/ZrO_2-MoO_3 catalysts were investigated, and emphasis was placed on both catalyst characterization and activity and selectivity of catalysts by performing reactions with modeling compounds (MCP and CH). The main conclusion of this work can be summarized as follows;

- XPS analysis showed that ZrO_2-MoO_3 catalysts can be prepared by the method of co-precipitation, and a good agreement of actual and theoretical Mo atomic percent was obtained. By analyzing the binding energies, molybdenum and zirconium compounds were present mainly in the form of MoO_3 and ZrO_2, respectively.
- XRD patterns showed that the crystal structure of ZrO_2 changed with the introduction of molybdenum. Pure zirconia showed very strong and dominant monoclinic characteristics. For catalyst with 4.7 at. % Mo, the mixture of monoclinic and tetragonal was observed, but relative intensity of tetragonal peak was greatly increased. Beyond that point, catalysts demonstrated similar signal, which was thought that ZrO_2 existed in the form of tetragonal phase.
- In the temperature range from ambient to 500 °C, reduction mainly occurred at two regions. Pure zirconia was not reducible during the studied temperature

range. Therefore, the two peaks were assigned to octahedral molybdenum species at low temperature and tetrahedral molybdenum species at high temperature. A three-peak spectrum was observed with the catalyst with 5 at. % Mo due to the formation of new molybdenum compound.

- The total acidity of catalysts was determined by NH_3-TPD. Three acidic sites were found in the series of catalysts. Each acidic site increased with the Mo content; however, the heat of desorption showed different trend. It reached the maximum value at catalyst containing 3.5 at. % Mo.
- BET surface area demonstrated the increasing tendency with Mo loading, which agreed with previous studies. The change can be explained that the introduction of Mo reduced the sintering and grain-growth rate of ZrO_2 by forming a two-dimensional layer on the surface of the zirconia particles.
- The catalysts containing Ir exhibited very high MCP conversion activity at 300°C and atmospheric pressure. Therefore, it can be concluded that the incorporation of iridium dramatically increased the activity. The variance of conversion was attributed to the difference of mechanisms. MCP followed the Hagg-Dessau mechanism on catalysts without Ir, while the classical bifunctional mechanism was prevailing for catalysts with Ir.
- Ir/ZrO_2-MoO_3 catalysts showed great activity and selectivity for the reaction of cyclohexane at high pressure and high temperature in a batch reactor. The cyclohexane was converted into products consisting of SRO products (n-hexane), propane, butane and pentane. The catalyst with 3.5 at. % Mo and 30 ppmw Ir gave overall good activity and selectivity.

In general, the interaction of acidic and metallic sites determines the performance of the catalysts. In order to acquire desirable activity and selectivity, the two functionalities must be balanced.

6.2 Future Work

The work done to date was centered on characterization of catalysts containing iridium and selective ring opening reaction with molecules like MCP and MH, which have simple structure and are favorable to SRO, so more future work is expected.

Different reaction parameters, such as temperature, hydrogen pressure, the ratio of reactant to catalyst, and reaction duration, will be chosen for SRO reaction of cyclohexane over the catalyst with 3.5 at. % and 30 ppmw Ir. The best parameters will be determined based on the activity and selectivity. The obtained conclusions will be verified by running experiments on a fixed-bed reactor. The effect of iridium size to activity and selectivity will also be investigated.

In addition, complex compounds, like benzene, alkylaromatics and tetralin, should be used to evaluate the performance of the bifunctional catalyst. In order to suppress the side reactions, the promoters, Ni, Co, may be incorporated.

REFERENCES

A.K. Aboul-Gheit, S.M. Aboul-Fotouh, N.A.K. Aboul-Gheit, "Effect of combining palladium, iridium or rhenium with platinum supported on H-ZSM-5 zeolite on their cyclohexene hydroconversion activities", Applied Catalysis A: General 292 (2005) 144-153.

A. Abraham, "Density-Functional Theory Study of Methylcyclohexane Selective Ring Opening over ZrO_2", Master Thesis, University of Alberta, 2005.

P. Afanasiev, C. Geantet, M. Breysse, "Preparation of High-Surface-Area Mo/ZrO_2 Catalysts by a Molten Salt Method: Application to Hydrodesulfurization", Journal of Catalysis 153 (1995) 17-24.

S. Albertazzi, R. Ganzerla, C. Gobbi, M. Lenarda, M. Mandreoli, E. Salatelli, P. Savini, L. Storaro, A. Vaccari, "Hydrogenation of naphthalene on noble-metal-containing mesoporous MCM-41 aluminosilicates", Journal of Molecular Catalysis A: Chemical 200 (2003) 261-270.

W.E. Alvarez, D.E. Resasco, "Methylcyclopentane ring opening as a reaction test for Pt catalysts supported on non-acidic materials", Journal of Catalysis. 164 (1996) 467-476.

M.A. Arribas, P. Concepcion, A. Martinez, " The role of metal sites during the coupled hydrogenation and ring opening of tetralin on bifunctional Pt(Ir)/USY catalysts", Applied Catalysis A: General 267 (2004) 111-119.

M.A. Arribas, A. Corma, M.J. Diaz-Cabanas, A. Martinez, "Hydrogenation and ring opening of tetralin over bifunctional catalysts based on the new ITQ-21 zeolite", Applied Catalysis A: General 273 (2004) 277-286.

M.A. Arribas, A. Martinez, "The influence of zeolite acidity for coupled hydrogenation and ring opening of 1-methylnaphthalene on Pt/USY catalysts", Applied Catalysis A: General 230 (2002) 203-217.

AutoChem II 2920 Automated Catalyst Characterization System Operator's ManualV2.00, Norcross, GA (2003).

AD. Bank, Policy guidelines for reducing vehicle emissions in Asia-Cleaner fuels, Asian Development Bank, 2003 p.44.

T. Bhaskar, K.R. Reddy, C.P. Kumar, M.R.V.S. Murthy, K.V.R. Chary, "Characterization and reactivity of molybdenum oxide catalysts supported on zirconia", Applied Catalysis A: General 211 (2001) 189-201.

G. Blyholder, "Molecular orbital view of chemisorbed carbon monoxide", Journal of Physical Chemistry, 68 (1964) 2772-2778.

B.H. Cooper, B.B.L. Donnis, "Aromatic saturation of distillates: an overview", Applied Catalysis A: General 137 (1996) 203-223.

A. Calafat, L. Avilan, J. Aldana, "The influence of preparation conditions on the surface area and phase formation of MoO_3/ZrO_2 catalysts', Applied Catalysis A: General 201 (2000) 215-223.

M. Che, C.O. Bennett, "M. Che, C.O. Bennett, Advances in Catalysis", Advances in Catalysis, 36 (1989) 55-172.

J. Cinibulk, Z. Vit, "Hydrodenitrogenation of pyridine over alumina-supported iridium catalysts", Applied Catalysis A: General, 180 (1999) 15-23.

A.Corma, V. González-Alfaro and A.V. Orchillés, "Decalin and tetralin as probe molecules for cracking and hydrotreating the light cycle oil", Journal of Catalysis, 200 (2001) 34-44.

D.S. Cunha, G.M. Cruz, "Hydrogenation of benzene and toluene over Ir particles supported on γ -Al_2O_3", Applied Catalysis A: General 236 (2002) 55-66.

H. Du, C. Fairbridge, H. Yang, Z. Ring, "The chemistry of selective ring-opening catalysts", Applied Catalysis A: General 294 (2005) 1-21.

D. Eliche-Quesada, J.M. Robles, P.M. Torres, E.R. Castellon, A.J. Lopez, "Superficial characterization and hydroconversion of tetralin over NiW sulfide catalysts supported on zirconium doped mesoporous silica", Applied Catalysis A: General 262 (2004) 111-120.

M. G. Falco, J. M. Grau, N. S. Figoli, "Platinum over tungsten oxide or sulfate promotedzirconia: a study of the metallic and acid functionsand their poisoning", Applied Catalysis A: General 264 (2004) 183-192.

F. Figueras, B. Coq, C. Walter, J. Y. Carriat, "Hydroconversion of methylcyclohexane on bifunctional sulfated zirconia-supported platinum catalysts", Journal of Catalysis, 169 (1997) 103-113.

T. Fujikawa, K. Idei, T. Ebihara, H. Mizuguchi, K. Usui, "Aromatic hydrogenation of distillates over SiO_2-Al_2O_3 supported noble metal catalysts", Applied Catalysis A: General 192 (2000) 253-261.

L.B. Galperin, J.C. Bricker, J.R. Holmgren, "Effect of support acid-basic properties on activity and selectivity of Pt catalysts in reaction of methylcyclopentane ring opening", Applied Catalysis A: General 239 (2003) 297-304.

F.G. Gault, "Mechanisms of skeletal isomerization of hydrocarbons on metals ", Advances in Catalysis, 30 (1981) 1-95.

R. Gopalan, C.-H. Chang, Y.S. Lin, "Thermal stability improvement on pore and phase structure of sol-gel derived zirconia", Journal of Materials Science, 30 (1995) 3075-3081.

D. Hamon, M. Vrinat, M. Breysse, B. Durand, M. Jebrouni, M. Roubin, P. Magnoux, T. Des Courieres, " Molten salt preparation of stabilized zirconia catalysts : characterization and catalytic properties", Catalysis Today, 10 (1991) 613-627.

Handbook of X-ray Photoelectron Spectroscopy, Perkin-Elmer Corporation, 1992.

R. Hoffmann, "Solids and surfaces: A Chemist's View of Bonding in Extended Structures", VCH Publisher, New York, 1988.

M. Jacquin , D.J. Jones, J. Rozière , A.J. López, E.R. Castellón, J.M.T. Menayo, M. Lenarda, L. Storaro, A. Vaccari, S. Albertazzi, "Cetane improvement of diesel with a novel bimetallic catalysts", Journal of Catalysis, 228 (2004) 447-459.

C. Kenney, "Characterization of ZrO_2-MoO_3 catalysts", Master Thesis, University of Alberta, 2004.

C. Kenney, Y. Maham, A.E. Nelson, "Characterization of monofuctional ZrO_2-MoO_3 catalysts for methylcyclopentane conversion", Thermochimica Acta, 434 (2005) 55-61.

C. Knottenbelt, "Mossgas 'gas-to-liquid' diesel fuels—an environmentally friendly option", Catalysis Today 71 (2002) 437–445.

R. Kramer, H. Zuegg, "The hydrogenolysis of methylcyclopentane on platinum model catalysts: Particle size effect due to a reaction occurring at the phase boundary metal-support ", Journal of Catalysis 80 (1983) 446-456.

R. Kramer, H. Zuegg, "The hydrogenolysis of methylcyclopentane on platinum model catalysts II. Particle size effect on Pt/SiO_2 catalysts due to adlineation of platinum and silica", Journal of Catalysis 85 (1984) 530-535.

D. Kubicka, N. Kumar, P. Mäki-Arvela, M. Tiitta, V. Niemi, T. Salmi, D.Yu. Murzin, "Ring opening of decalin over zeolites I. activity and selectivity of proton-form zeolites", Journal of Catalysis 222 (2004A) 65-79.

D. Kubicka, N. Kumar, P. Maki-Arvela, M. Tiitta, V. Niemi, H. Karhu, T. Salmi, D.Yu. Murzin, "Ring opening of decalin over zeolites II. activity and selectivity of platinum-modified catalysts", Journal of Catalysis 227 (2004B) 313-327.

L.M. Kustov, A.Yu. Stakheev, T.V. Vasina, O.V. Masloboishchikova, E.G. Khelkovslaya-Sergeeva and P. Zeuthen, Studies in surface science and catalysis 138 (2001) 307.

SL Lee, W. MD, PH. Desai, CC. Jonhnson, MY. Asim, "Aromatics reduction and cetane improvement of diesel fuels", Fuel Reformulation 3 (1993) 26–31.

S.K. Maity, M.S. Rana, B.N. Srinivas, S.K. Bej, G. Murali Dhar, T.S.R. Prasada Rao, "Characterization and evaluation of ZrO2 supported hydrotreating catalysts", Journal of Molecular Catalysis A: Chemical 153 (2000) 121-127.

RL. McCormick, JR. Alvarez, MS. Graboski, "NO_x solutions for biodiesel in 2003", Colorado Institute for Fuels and Engine Research, C.S.O.M.G.,Colorado, NREL, (2003) 1–39.

G.B. McVicker, M. Daage, M.S. Touvelle, C.W. Hudson, D.P. Klein, W.C. Baird, B.R. Cook, J.G. Chen, S. Hantzer, D.E.W. Vaughan, E.S. Ellis and O.C. Feeley, "Selective ring opening of naphthenic molecules", Journal of Catalysis 210 (2002) 137-148.

R. Navarro, B. Pawelec, J.L.G. Fierro, P.T. Vasudevan, J.F. Cambra, P.L. Arias, "Deep hydrodesulfurization of DBT and diesel fuel on supported Pt and Ir catalysts", Applied Catalysis A: General 137 (1996) 269-286.

U.Nylen, J. F. Delgado, S. Jaras, M. Boutonnet, "Low and high-pressure ring opening of indan over 2 wt. % Pt, Ir and bi-metallic Pt25Ir75/boehmite catalysts prepared from microemulsion systems", Applied Catalysis A: General 262 (2004) 189-200.

T. Ono, H. Kamisuki, H. Hisashiand, H. Miyata, "A comparison of oxidation activities and structures of Mo oxides highly dispersed on group IV oxide supports", Journal of Catalysis 116 (1989) 303-307.

Z. Paal, D. Teschner, N.M. Rodriguez, R.T.K. Baker, L. Toth, U. Wild, R. Schlogl, "Rh/GNF catalysts: characterization and catalytic performance in methylcyclopentane reactions", Catalysis Today 102-103 (2005) 254-258.

A. Raichle, Y. Traa, F. Fuder, M. Rupp, J. Weitkamp, "Haag-Dessau catalysts for ring opening of cycloalkanes", Angew. Chem. Int. Ed. 2001, 40, No.7.

A. Raichle, Y. Traa, J. Weitkamp, "Producing a high-quality synthetic steamcracker feedstock from different aromatic model components of pyrolysis gasoline on bifunctional zeolite catalysts", Catalysis Today 75 (2002) 133-139.

F. Roessner, U. Roland, "Hydrogen spillover in bifunctional catalysis", Journal of Molecular Catalysis A: Chemical 112 (1996) 401-412.

M. Santikunaporn, J.E. Herrera, S. Jongpatiwut, D. E. Resasco, W. E. Alvarez, E. L. Sughrue, "Ring opening of decalin and tetralin on HY and Pt/HY zeolite catalysts", Journal of Catalysis 228 (2004) 100-113.

C.Song, X. Ma, "New design approaches to ultra-clean diesel fuels by deep desulfurization and deep dearomatization », Applied Catalysis B: Environmental 41 (2003) 207-238.

D. Teschner, K. Matusek, Z. Paal, "Ring opening of methylcyclopentane on alumina-supported Rh catalysts of different metal loadings", Journal of Catalysis 192 (2000) 335-343.

D. Teschner, Z. Paal, D. Duprez, "The effects of hydrogen pressure and temperature on the methylcyclopentane conversion on Rh catalysts", Catalysis Today 65 (2001) 185-190.

D. Teschner, L. Pirault-Roy, D. Naud, M. Guerin, Z. Paal, "Methylcyclopentane reactions on Rh-Ge/Al_2O_3 catalysts prepared by controlled surface reaction", Applied Catalysis A: General 252 (2003) 421-426.

C.G. Walter, B. Coq, F. Figueras, M. Boulet, "Competitive reation of methylcyclohexane and n-hexane over alumina-supported platium, iridium and ruthenium catalysts", Applied Catalysis A: General 133 (1995) 95-102.

O. Weisser, S. Landa, Sulphide Catalysts-their properties and applicatioins, Pergamon Press, Oxford.

J. Weitkamp, A. Raichle, Y. Traa, "Novel zeolite catalysis to create value from surplus aromatics: preparation of C_{2+} n-alkanes, a high-quality synthetic steamcracker feedstock", Applied Catalysis A: General 222 (2001) 277-297.

S. Xie, K. Chen, A.T. Bell, E. Iglesia, "Structural characterization of molybdenum oxide supported on zirconia", Journal of Physical Chemistry B 104 (2000) 10059-10068.

H. Yasuda, T. Sato, Y. Yoshimura, "Influence of the acidity of USY zeolite on the sulfur tolerance of Pd–Pt catalysts for aromatic hydrogenation", Catalysis Today 50 (1999) 63-71.

H. Yasuda, Y. Yoshimura, "Hydrogenation of tetralin over zeolite-supported Pd-Pt catalysts in the presence of dibenzothiophene", Catalysis Letters 46 (1997) 43-48.

F. Zaera, "Probing catalytic reactions at surfaces", Progress in Surface Science 69 (2001) 1-98.

B. Zhao, X. Xu, H. Ma, D. Sun, J. Gao, "Monolayer dispersion of oxides and salts on surface of ZrO_2 and its application in preparation of ZrO_2-supported catalysts with high surface areas", Catalysis Letters 45 (1997) 237-244.

Y. Zhuang, A. Frennet, "Kinetic studies of methylcyclopentane ring opening on EuroPt-1 (Pt/SiO_2)", Applied Catalysis A: General 177 (1999) 205-217.

WEBSITES

http://www.energy.gov.ab.ca/docs/oilsands/pdfs/osgenbrf.pdf Viewed on September 13, 2005

http://www.energy.gov.ab.ca/docs/aboutus/pdfs/Alberta_Energy_Overview.pdf Viewed on September 13, 2005

http://www.alberta-canada.com/economy/naturalAdvantages/energy.cfm Viewed on September 13, 2005

http://www.capp.ca/raw.asp?x=1&dt=NTV&e=PDF&dn=34093 Viewed on September 13, 2005

http://www.energy.gov.ab.ca/89.asp Accessed date: September 13, 2005

http://www.epa.gov/fedrgstr/EPA-AIR/2001/January/Day-18/a01a.pdf Viewed on July 21, 2005

http://www.epa.gov/fedrgstr/EPA-AIR/2004/June/Day-29/a11294.pdf Viewed on July 21, 2005

http://www.dieselnet.com/standards/eu/ld.html Viewed on July 22, 2005

http://www.dieselnet.com/gl-a.html Viewed on July 30, 2005

http://www.lenntech.com/zeolites-structure-types.htm Viewed on September 18, 2005

http://www.accuratus.com/zirc.html Viewed on January 21, 2005

http://www.americanelements.com/newpage3.htm Viewed on January 21, 2005

http://www.missouri.edu/~murrwww/pages/ac_naa2.shtml Viewed on October 3, 2005

http://www.micromeritics.com/products/autochem_overview.aspx?id=94 Viewed on October 5, 2005

http://www.panalytical.com/index.cfm?pid=147 Viewed on October 6, 2005

http://srdata.nist.gov/xps/Bind_E.asp View on February 13, 2006

http://webbook.nist.gov/cgi/cbook.cgi?Name=methylcyclopentane&Units=SI&cMS=on Viewed on June 26, 2006